164
BNL 585 (T-146)
(Reactors – General)
(Metallurgy and Ceramics)

CORROSION STUDIES FOR A FUSED SALT-LIQUID METAL EXTRACTION PROCESS FOR THE LIQUID METAL FUEL REACTOR

H. SUSSKIND, F.B. HILL, L. GREEN, S. KALISH, L.E. KUKACKA,
W.E. MCNULTY, AND E. WIRSING, JR.

June 30, 1960

BROOKHAVEN NATIONAL LABORATORY
Associated Universities, Inc.
under contract with the
United States Atomic Energy Commission

CORROSION STUDIES FOR A FUSED SALT-LIQUID METAL EXTRACTION PROCESS FOR THE LIQUID METAL FUEL REACTOR*

H. SUSSKIND, F.B. HILL, L. GREEN, S. KALISH, L.E. KUKACKA,
W.E. MCNULTY, AND E. WIRSING, JR.

June 30, 1960

*A condensed version of this report appeared in *Chemical Engineering Progress* **56**, 57-63 (1960).

BROOKHAVEN NATIONAL LABORATORY
Upton, N. Y.

LEGAL NOTICE

PRINTED IN USA
PRICE $1.00

Available from the
Office of Technical Services,
Department of Commerce
Washington 25, D.C.

March 1961 975 copies

ABSTRACT

Corrosion screening tests have been carried out on potential materials of construction for use in a fused salt – liquid metal extraction process plant. The work was done in support of the Liquid Metal Fuel Reactor fuel processing project. The corrodents of interest were NaCl-KCl-$MgCl_2$ eutectic, LiCl-KCl eutectic, Bi-U fuel, and $BiCl_3$, either separately or in various combinations. Screening tests to determine the resistance of a wide range of commercial alloys to these corrodents were performed in static and tilting-furnace capsules. Some ceramic materials were also tested in static capsules. Larger-scale tests of metallic materials were conducted in thermal convection loops and in a forced circulation loop. Some of these tests were conducted isothermally at 500°C, and others were performed under 40° to 50°C temperature differences at roughly the same temperature level. On the basis of metallographic examination of exposed test tabs and chemical analyses of corrodents, it was found that the binary and ternary eutectics by themselves produced little attack on any of the materials tested. A wide variety of materials including 1020 mild steel, 2¼ Cr – 1 Mo alloy steel, types 304 (ELC), 310, 316, 347, 430, and 446 stainless steel, 16-1 Croloy, Inconel, Hastelloy C, Inor-8, Mo, and Ta is, therefore, available for further study. Corrosion by the ternary salt – fuel system was characteristic of that produced by the fuel alone. Alloys such as 1020 mild steel, and 1¼ Cr – ½ Mo and 2¼ Cr – 1 Mo alloy steel, which are resistant to fuel, therefore, would be likely choices at present for container materials. $BiCl_3$ produced extensive attack on ternary salt – fuel containers when the fuel contained insufficient concentrations of oxidizable solutes. Au and Al_2O_3 were the only materials not attacked by $BiCl_3$ in ternary salt alone.

CONTENTS

Introduction 1

Experimental Program 2

Preparation and Handling of Corrodents 3

Test Specimen Preparation 3

Specimen Examination and Corrodent Analysis 3

Static Tests 4

LiCl-KCl Eutectic 4

NaCl-KCl-$MgCl_2$ Eutectic 4

$BiCl_3$ 4

Effect of Radiation 4

Tilting-Furnace Capsule Tests 6

NaCl-KCl-$MgCl_2$ Eutectic Tests 12

Bi-U Fuel/Ternary Eutectic Tests 13

Ternary Eutectic/$BiCl_3$ and Bi-U Fuel/Ternary Eutectic/$BiCl_3$ Tests 16

Thermal Convection Loop Tests 16

Loop F 19

Loop L-1 20

Loop L-3 20

Loop L-5 20

CONTENTS

Loop L-6 21

Loop L-7 21

Forced Circulation Loop Test 22

Summary of Results 23

Acknowledgments 24

References 25

Appendix A. Mill Test Reports of Metallic Materials Tested 27

Appendix B. Chemical Analysis of Bi-U Fuel and Fused Salt Solutions 28

Appendix C. Axial Temperature Profile of Tilting-Furnace Capsule 29

Appendix D. Crimping Forces Used in Tilting-Furnace Capsule Preparation 30

Appendix E. Test Data and Results for Tilting-Furnace Capsule Screening Tests 31

Corrodent: $NaCl\text{-}KCl\text{-}MgCl_2$ Eutectic 31

Welded Tab Specimens; Corrodent: $NaCl\text{-}KCl\text{-}MgCl_2$ Eutectic 33

Corrodent: Bi-U Fuel and Ternary Eutectic 34

Corrodent: $NaCl\text{-}KCl\text{-}MgCl_2$ Eutectic Plus 4.76% $BiCl_3$ 38

Corrodent: Bi-U Fuel/Ternary Eutectic Plus 4.76% $BiCl_3$ 39

Appendix F. Results of Thermal Convection and Forced Convection Loop Corrosion Product Analyses 40

CORROSION STUDIES FOR A FUSED SALT-LIQUID METAL EXTRACTION PROCESS FOR THE LIQUID METAL FUEL REACTOR

INTRODUCTION

A typical fuel for use in a Liquid Metal Fuel Reactor (LMFR) is a dilute solution of U, Mg, and Zr in Bi. By means of a process which has been under development at Brookhaven National Laboratory,[1] an important group of fission products may be continuously removed from the fuel by contacting it with a mixture of fused chlorides at 450° to 500°C. A small portion of the fuel stream is continuously fed to an extraction column (No. 1 in Figure 1) in which it is contacted with the fused eutectic mixture of NaCl, KCl, and $MgCl_2$ (30, 20, and 50 mole %, respectively; m.p. 396°C). A small amount of the strong oxidant $BiCl_3$ is added to the influent salt. Those fission products (identified as FPS in Figure 1) whose chlorides are more stable than $MgCl_2$ and some U are oxidized into the salt in this column. Make-up Mg is added to the fuel before it is returned to the reactor. U in the salt leaving column 1 is recovered first by reduction into a solution of Mg in Bi in column 2. It is then oxidized into the incoming salt by $BiCl_3$ in column 3.

It is apparent that the corrosion environment in such a processing plant would vary considerably from one point to another. Certain vessels and piping would be exposed to highly oxidizing $BiCl_3$ solutions, and others would be exposed only to the relatively inert NaCl-KCl-$MgCl_2$ eutectic. Some components would be exposed to the molten fuel alone and others to the ternary salt alone. Con-

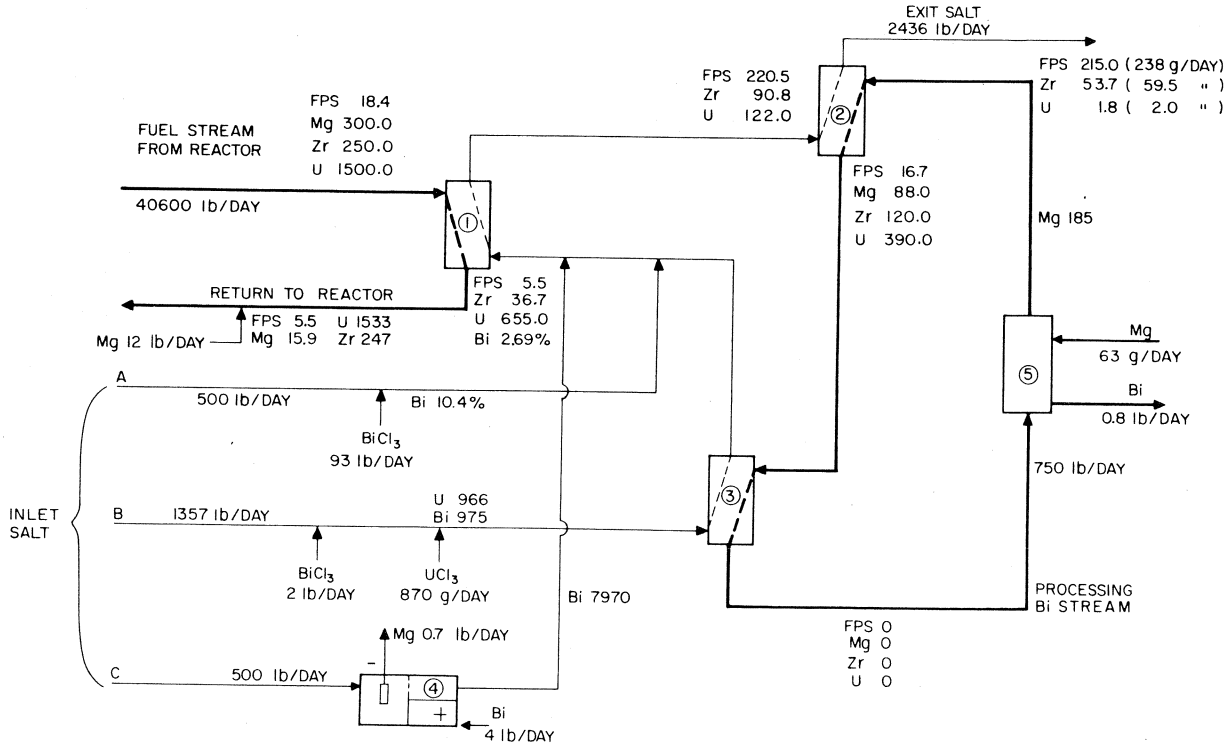

Figure 1. Process flow sheet for LMFR fused salt extraction of fission products from Bi-U fuel.[1] FPS denotes fission products. Concentrations are in ppm unless otherwise indicated.

tacting vessels would contain both fuel and salt in two-phase flow. Fission product decay heat might give rise to temperature gradients resulting in mass transfer corrosion.

The purpose of the work described in this paper was to perform corrosion screening tests on materials of construction for an LMFR fuel processing plant. The testing program was not completed because of phase-out of work on fluid-fuel reactor concepts.[2] The principal results of the program are reported here. Most of the work was in support of a process design based on the NaCl-KCl-$MgCl_2$ eutectic.[1] Some work is reported on the LiCl-KCl eutectic (41 mole % KCl, m.p. 351°C) which was the salt first used in fuel processing studies at BNL.[3]

Previous Work

Corrosion by the liquid metal fuel itself was the subject of a separate program at BNL,[4] and hence no fuel corrosion tests *per se* were performed in the work described here. In the fuel corrosion program, most experience was obtained with a fuel composed of 1000 ppm U, 350 ppm Mg, and 250 to 350 ppm Zr in Bi. Mg was present as a getter to protect U from oxidation. Zr is believed to form a protective film of ZrN or ZrC on the container surface by reaction with N or C from the container material. This fuel has been circulated for many thousands of hours without causing serious corrosion in thermal convection loops and forced convection loops made of low-chrome alloy steels (1¼ Cr – ½ Mo and 2¼ Cr – 1 Mo) with temperature differences of up to 100°C and at maximum temperatures of 550°C. Although the various aspects of the corrosion resistance of these steels have not yet been fully studied, one of the following would most likely be specified at present as the fuel container material for any proposed reactor experiment: 1¼ Cr – ½ Mo, 2¼ Cr – 1 Mo, or 1020 mild steel.

Fused salts have been used industrially for many years, in pyrometallurgical refining processes and in heat transfer and metals heat treating applications. Yet few corrosion data have been published, especially on fused chloride systems. One of the few existing pertinent papers describes an extensive investigation of materials for molten chloride heat treating baths.[5] In this work it was found that intergranular penetration along carbide networks was far more important than general solution of metal. High-nickel, low-chrome alloys were found to offer the most resistance to corrosion in 50-hr static tests at 870°C.

With few data available for interpretation, theories of fused salt corrosion are largely speculative. Although substantial solubility of metals in their own salts has been noted,[6] corrosion by salts of metals different from the container material is thought to occur generally as a result of electrochemical action rather than by physical solution. Effects commonly associated with physical solution, such as mass transfer corrosion, are nevertheless possible if, in the corrosion mechanism, a temperature-dependent electrochemical equilibrium is involved.

No previous work seems to have been reported on corrosion by a two-phase liquid metal – fused salt system.

EXPERIMENTAL PROGRAM

The experimental program was designed to proceed from relatively simple and inexpensive small-scale static and tilting-furnace capsule tests to tests in recirculating thermal and forced convection loops which more closely approximate the conditions of flow and temperature distribution that might arise in a processing plant. Materials which showed promise in capsule-scale tests and were also practical from the point of view of availability, high temperature strength, ease of fabrication, or compatibility with fuel were tested in recirculating loops.

A list of the materials tested is given in Table 1. Mill test reports for the tests involving the ternary eutectic are given in Appendix A. The metallic materials tested included mild steel, ferritic and austenitic stainless steels, high-nickel alloys, Ta, and Mo. This wide range was selected because of the general lack of corrosion information on which to base a narrower one. Mo, Ta, and the ceramic materials were of special interest as potential container materials for $BiCl_3$ solutions.

The following corrodents were used: the NaCl-KCl-$MgCl_2$ eutectic, the same with 5% $BiCl_3$ added, and each of these in the presence of the liquid metal fuel. Pure $BiCl_3$ was used in one test, and LiCl-KCl eutectic was used by itself in an early series of tests. Generally, the fuel and eutectic salt differed from what might be found in a processing plant principally in the absence of radiation and fission products. The effect of gamma radiation was determined in one experiment, but the effect

of fission products had not been examined before the corrosion study was terminated.

Before discussion of the tests, a description is given below of certain experimental procedures used in most of them.

Preparation and Handling of Corrodents

It was essential that all purification and handling of purified corrodents in the liquid state be performed in an inert atmosphere, since both the liquid metal fuel and the fused salts are subject to rapid attack by atmospheric moisture. Inert atmospheres were essential in the tests themselves for the same reason. In addition, corrosion by fused salts is greatly enhanced by the presence of oxidizing impurities. Consequently, all apparatus for corrodent preparation or testing was thoroughly cleaned and tested for leak tightness (e.g., with a He mass spectrometer detector) before use. The inert atmospheres used were either He or Ar, purified by passage over Ti chips at 850°C.

Fuel that had been exposed to air in the solid state was slowly heated and melted under vacuum before use. Handling of purified solid salts was done in a dry box insofar as possible. Periods of handling in air outside a dry box were no longer than a few seconds and were immediately followed by evacuation and purging with He.

The eutectic salts were prepared by vacuum-melting the constituent salts in the proper proportions and outgassing at 500°C to a pressure of $<20\ \mu$ Hg. Reagent grade Baker LiCl, NaCl, and KCl, General Chemical $BiCl_3$, and Carborundum Metals Co. anhydrous $MgCl_2$ were used. Small batches of salt for the static tests were prepared in Pyrex, and 100-lb batches for the other experiments in 347 stainless steel tanks. In the latter case, the binary and ternary salts were contacted with Bi containing 0.5% Mg, 0.5% U, and 0.025% Zr before use in order to reduce any oxides present into the Bi phase. The $BiCl_3$ was purified by vacuum sublimation at 225°C. Prior to use, the salts were filtered through fine Pyrex or stainless steel frits.

The Bi, 99.999% pure, was degreased with acetone and dried. Spectrographically pure Johnson, Matthey Mg and reactor grade Zr from Zirconium Metals Co. were degreased with acetone, and natural U was cleaned with nitric acid to remove surface oxides and also degreased with acetone. The Bi fuel, containing 1000 ppm U, 350 ppm Mg, and 350 ppm Zr, was prepared by dissolving weighed quantities of these additives in the Bi at 500°C with light vibration of the container.

Table 1

Materials Tested

Metals and Alloys		
1020 Mild steel	347 S.S.	Inor-8
1¼ Cr – ½ Mo steel	410 S.S.	Hastelloy C
2¼ Cr – 1 Mo steel	430 S.S.	Tantalum
5 Cr steel	16-1 Croloy	Molybdenum
304 (ELC) S.S.	446 S.S.	Gold
310 S.S.	Inconel	Stellite 90
316 S.S.		

Ceramics
Al_2O_3 (Norton Co. Mix A-402)
MgO (Norton Co. Mix M-202)
ZrO_2 (Norton Co. Mix Z-301)
SiC (nitride bonded)

Test Specimen Preparation

Flat metal tab specimens were used in the static and tilting-furnace experiments. One face was mechanically polished and the other electropolished or sandblasted to simulate possible surface cleaning treatments. Each specimen was weighed before testing. The loop test specimens were polished lengths of pipe welded directly into the flow circuit. A short section of each such specimen was set aside for reference. Specimens for the tilting-furnace and loop tests were prepared from the same stock as that used in fabrication of the container. Ceramic tabs were dried to constant weight at 200°C before use.

Specimen Examination and Corrodent Analysis

On completion of the tests, each tilting-furnace capsule and thermal convection loop was radiographed to determine the location and extent of gross corrosion and deposition. Then, for all tests, test specimens were recovered and washed with distilled water to remove all traces of adhering salt. Ceramic specimens were refluxed with distilled water and dried to constant weight at 200°C. Adhering Bi was removed from tab surfaces by dissolution in Hg at 200°C. All capsule specimens were then weighed. Metallic specimens were examined metallographically to determine the type and extent of corrosion. Maximum depth of specimen penetration was measured on photomicrographs. Ceramic specimens were examined

visually. Whenever possible, the corrodent solution and any plug material were analyzed chemically (Appendix B).

Capsule-scale experiments involved two to four replicate capsules for a given material. Although there was considerable scatter within groups of measured weight changes and depths of penetration for a given material, cases of substantial corrosion were clearly evident.

In the following sections, the tests are described and the results given in order of increasing size of the test apparatus used.

STATIC TESTS

Fifteen-gram batches of salt were weighed out in a dry box and placed in Pyrex capsules with ⅜ × ⅜ × 0.030-in. test specimens. The capsules were sealed under vacuum and placed in a furnace maintained at 500°C. The tests were performed in quadruplicate for 1000 hr.

LiCl-KCl Eutectic

The results are shown in Table 2. Types 347 and 410 stainless steel offered the best corrosion resistance to the salt. Cr – 5 Si steel, W, and Mo suffered such slight attack that it could not be measured at a magnification of 250×. The 2¼ Cr – 1 Mo steel showed intergranular attack of 0.3 mil; 5 Cr steel suffered from local transgranular and intergranular attack of 0.5 mil; and Ta pitted to a maximum depth of 0.9 mil.

In addition to undergoing the capsule test, type 410 stainless steel was also statically exposed to the binary salt in the surge tank of a thermal convection loop (L-2) in which U-Bi solution was circulated.[7] No corrosion was observed after 3810 hr of exposure at 550°C

Table 2

Results of Static Screening Tests

Test duration: 1000 hr
Test temperature: 500°C
Corrodent: LiCl-KCl eutectic

Material	Type of corrosion	Max. penetration,* mils/yr
2¼ Cr – 1 Mo steel	Intergranular	2.6
5 Cr steel	Local intergranular and transgranular	4.4
Cr – 5 Si steel	Intergranular	<0.44
347 S.S.	None	0
410 S.S.	None	0
Tungsten	Intergranular	<0.44
Molybdenum	Intergranular	<0.44
Tantalum	Pitting	7.9

*Average of 2 tests.

$NaCl-KCl-MgCl_2$ Eutectic

Twelve metallic and four ceramic materials were exposed to the eutectic and to a solution of 5% $BiCl_3$ in the eutectic in static corrosion tests.

The results are presented in Tables 3 and 4. 5 Cr steel pitted, and Ta suffered embrittlement. None of the other metals was seriously attacked by the eutectic. On the other hand, with the $BiCl_3$ solution, all the metallic specimens were severely corroded intergranularly and in some cases transgranularly as well (Figure 2). The 2¼ Cr – 1 Mo steel was pitted. All cases of attack were accompanied by significant weight losses and almost complete reduction of the $BiCl_3$. The original surfaces of the metallic specimens were completely dissolved.

Al_2O_3 was the only ceramic tested which was not attacked by either the eutectic or a solution of $BiCl_3$ in the eutectic. In both cases, MgO and ZrO_2 cracked and spalled to some extent, while the nitride-bonded SiC crumbled completely. Although there was some loss of $BiCl_3$, particularly with MgO, no metallic Bi was found.

$BiCl_3$

Several 1000-hr static tests were performed in Pyrex capsules at 300°C to determine the resistance of Mo to a solution of pure $BiCl_3$. No attack or weight change was observed on any of the specimens.

Effect of Radiation

One experiment was performed to determine the effect of gamma radiation on ternary salt corrosion. An evacuated, glass-lined, stainless steel capsule (Figure 3) was filled with ternary eutectic, and three polished and weighed type 347 stainless steel test tabs were immersed in it. Temperature was measured with a thermocouple inserted in a stainless steel thermowell. The thermowell was covered with a glass liner with attached hooks on which the test tabs were hung. The capsule was filled with salt charged directly from the purification

Table 3

Results of Static Screening Tests* of Metals and Alloys

Test duration: 1000 hr
Test temperature: 500°C

Material	Corrodent: $NaCl-KCl-MgCl_2$ eutectic — Type of corrosion	Max. penetration, mils/yr	Approx. weight change, %	Corrodent: $NaCl-KCl-MgCl_2$ eutectic plus 5% $BiCl_3$ — Type of corrosion	Approx. weight change, %	Residual % $BiCl_3$ in salt
1020 Mild steel	None	0	−0.4	Intergranular	−8	0.61
1¼ Cr – ½ Mo steel		†		Intergranular	−20	0.30
5 Cr steel	Pitting	17.5	‡		†	
2¼ Cr – 1 Mo steel	Intergranular	<1	−2.6	Pitting	−14	0
347 S.S.	Intergranular	1	−0.6	Intergranular	−30	0
430 S.S.		†		"	−21	0.33
16-1 Croloy		†		"	−22	0.30
446 S.S.	Intergranular	<1	−4.2	"	−27	0
Inor-8		†		"	−20	0.25
Stellite-90	Intergranular and transgranular	<1	−0.2	Intergranular and transgranular	−17.5	0
Molybdenum	None	0	0		†	
Tantalum	None**	0	0		†	

*Results are averages of 2 to 4 tests.
**Tab showed embrittlement.
†Not tested.
‡Not measured.

Table 4

Results of Static Screening Tests* of Ceramics

Test duration: 1000 hr
Test temperature: 500°C

Material	Corrodent: $NaCl-KCl-MgCl_2$ eutectic — Condition of specimen after test	Approx. weight change, %	Corrodent: $NaCl-KCl-MgCl_2$ eutectic plus 5% $BiCl_3$ — Condition of specimen after test	Approx. weight change, %	Residual % $BiCl_3$ in salt
Al_2O_3 (Norton Mix A-402)	No spalling or cracking	−0.14	No spalling or cracking	+ 0.3	4.5
MgO (Norton Mix M-202)	All specimens cracked and spalled	+6	All specimens cracked and spalled	+10	2.1
ZrO_2 (Norton Mix Z-301)	Moderately spalled	−1.6	Slight attack	+ 0.1	4.4
SiC (nitride bonded)	All specimens crumbled completely	—	All specimens crumbled completely	—	3.5

*Results are averages of 2 to 4 tests.

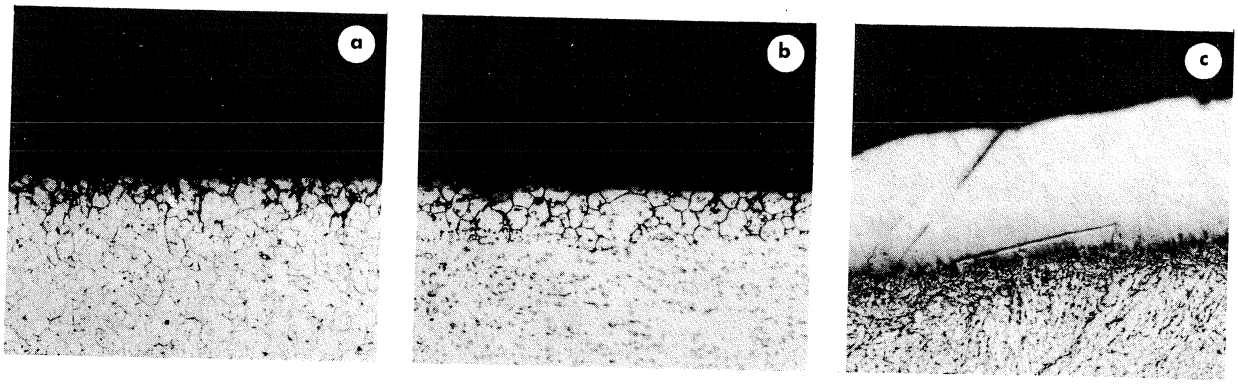

Figure 2. Photomicrographs (250×) of specimens exposed to static NaCl-KCl-$MgCl_2$ eutectic containing 5% $BiCl_3$ for 1000 hr at 500°C. Surfaces shown are polished sides of tabs. (a) Type 347 stainless steel; Marbles etch. (b) Type 446 stainless steel; HCl, picric acid, alcohol etch. (c) 2¼ Cr – 1 Mo alloy steel showing Bi deposit; nital etch.

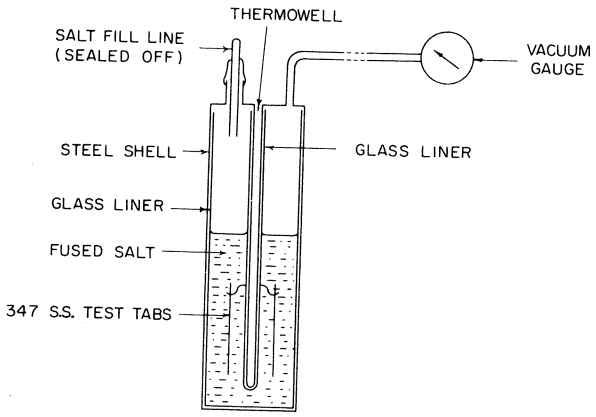

Figure 3. Schematic diagram of apparatus for salt corrosion test in a Co^{60} gamma radiation field.

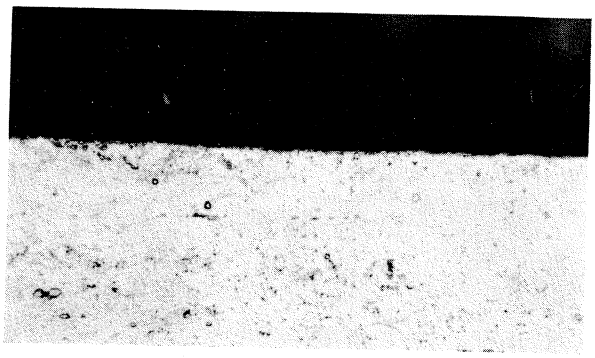

Figure 4. Photomicrograph (500×) of type 347 stainless steel specimen exposed to NaCl-KCl-$MgCl_2$ eutectic for 1050 hr at 500°C in a Co^{60} gamma radiation field. Salt dose rate: 183,000 r/hr. Specimen dose rate: 157,000 r/hr. Note deposit on polished surface. Marbles etch.

apparatus through a glass fill connection which was then sealed. A Calrod heater was wrapped around the outside of the capsule, and the whole unit insulated. A vacuum gauge was connected to the capsule. The capsule was exposed to a Co^{60} gamma radiation field for 1050 hr at 500°C. The salt was exposed to an average intensity of 183,000 r/hr and the steel tabs to 157,000 r/hr.

The lack of any measurable gas build-up within the capsule during the test indicated the absence of substantial salt decomposition. No corrosion was observed on the steel tabs, which still retained their metallographic polish at the end of the run.

A very thin film of a nonmetallic nature was observed on the lower part of the tabs (Figure 4). An unsuccessful attempt was made to identify this film by x-ray analysis. It is believed to be an oxide, and probably came from the salt.

TILTING-FURNACE CAPSULE TESTS

The tilting-furnace is a relatively simple apparatus for initial screening tests of materials for resistance to corrosion in the presence of flow and temperature differences. Because of its simplicity and the fact that both one- and two-phase corrodents could be accommodated, it was widely used in the present investigation.

The apparatus consisted of six furnaces mounted on a motor-driven tilting angle-iron framework (Figure 5). The furnaces were made from 18-in.-long, 1¾-in.-i.d. Mullite tubes (Figure 6)

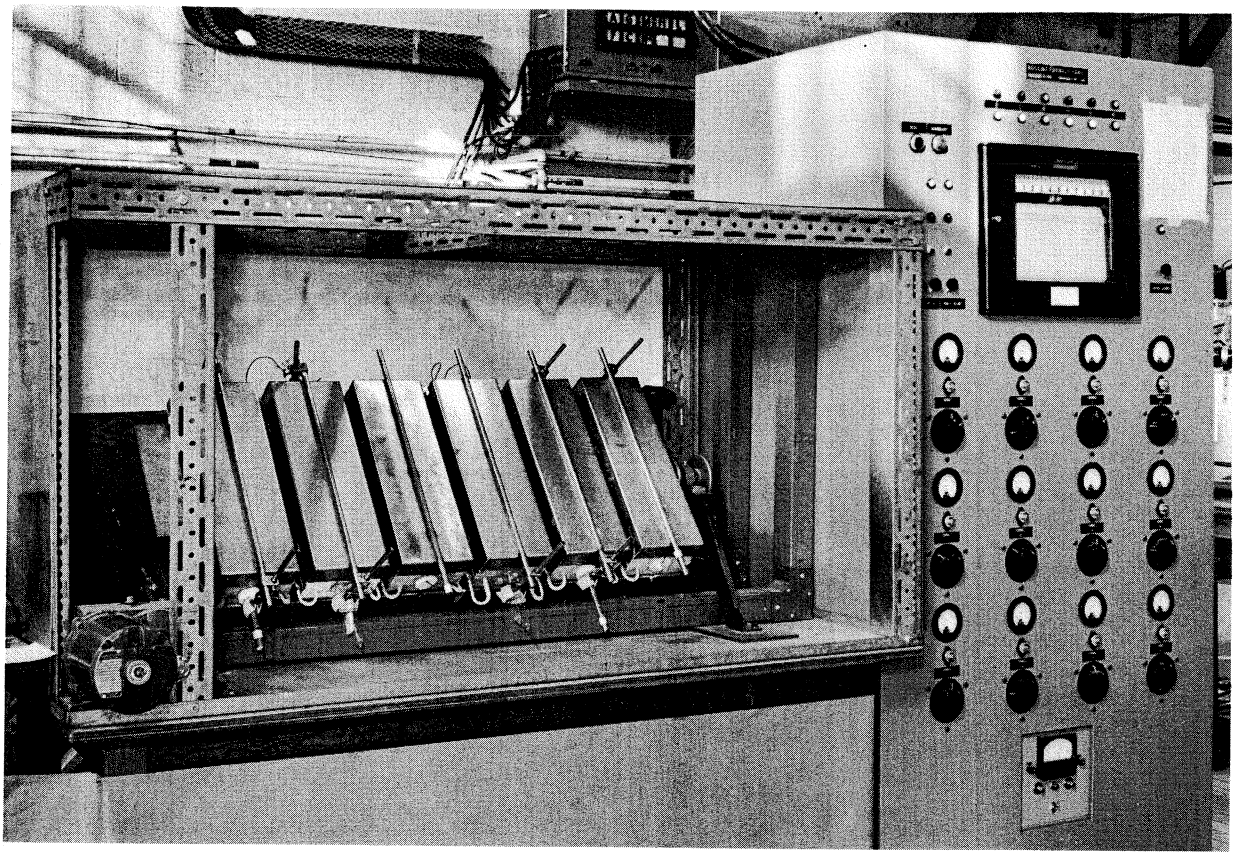

Figure 5. Tilting-furnace apparatus.

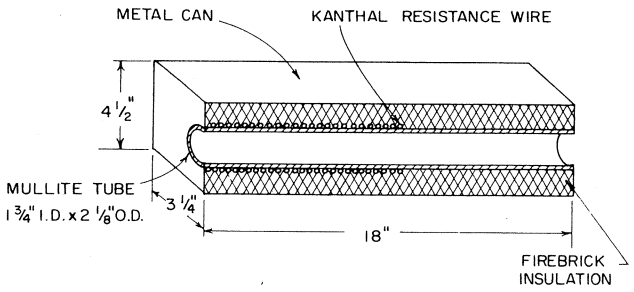

Figure 6. Schematic diagram of a tilting-furnace.

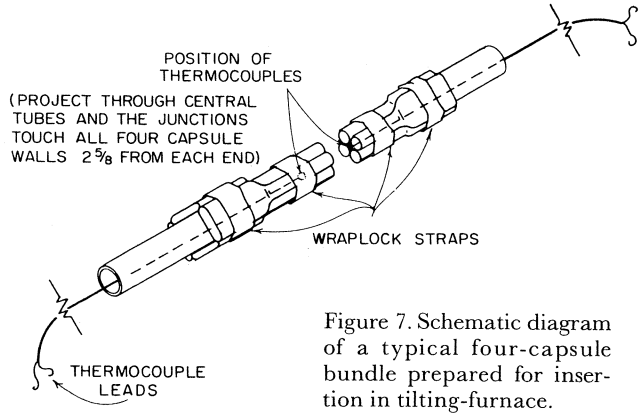

Figure 7. Schematic diagram of a typical four-capsule bundle prepared for insertion in tilting-furnace.

wound with Kanthal A resistance heater wire. One end of each tube was not wound with heater wire in order to promote an axial temperature gradient in capsules placed in the furnaces. Flow of corrodents within the capsules was obtained by slowly tilting the furnaces back and forth. The tilting cycle was 125 sec with a 37-sec delay at each extreme position to allow equilibration of the corrodent temperatures. To achieve this operation, the driving motor was interrupted and restarted by an air-operated time-delay, which was in turn actuated by a cam and microswitch arrangement on the angle-iron framework. The axial position of the capsules within the furnaces was adjusted so that the cold ends were maintained at 450°C while the hot ends were controlled at 500°C by a thermocouple and temperature recorder controller. Tests were carried out in duplicate for 1000

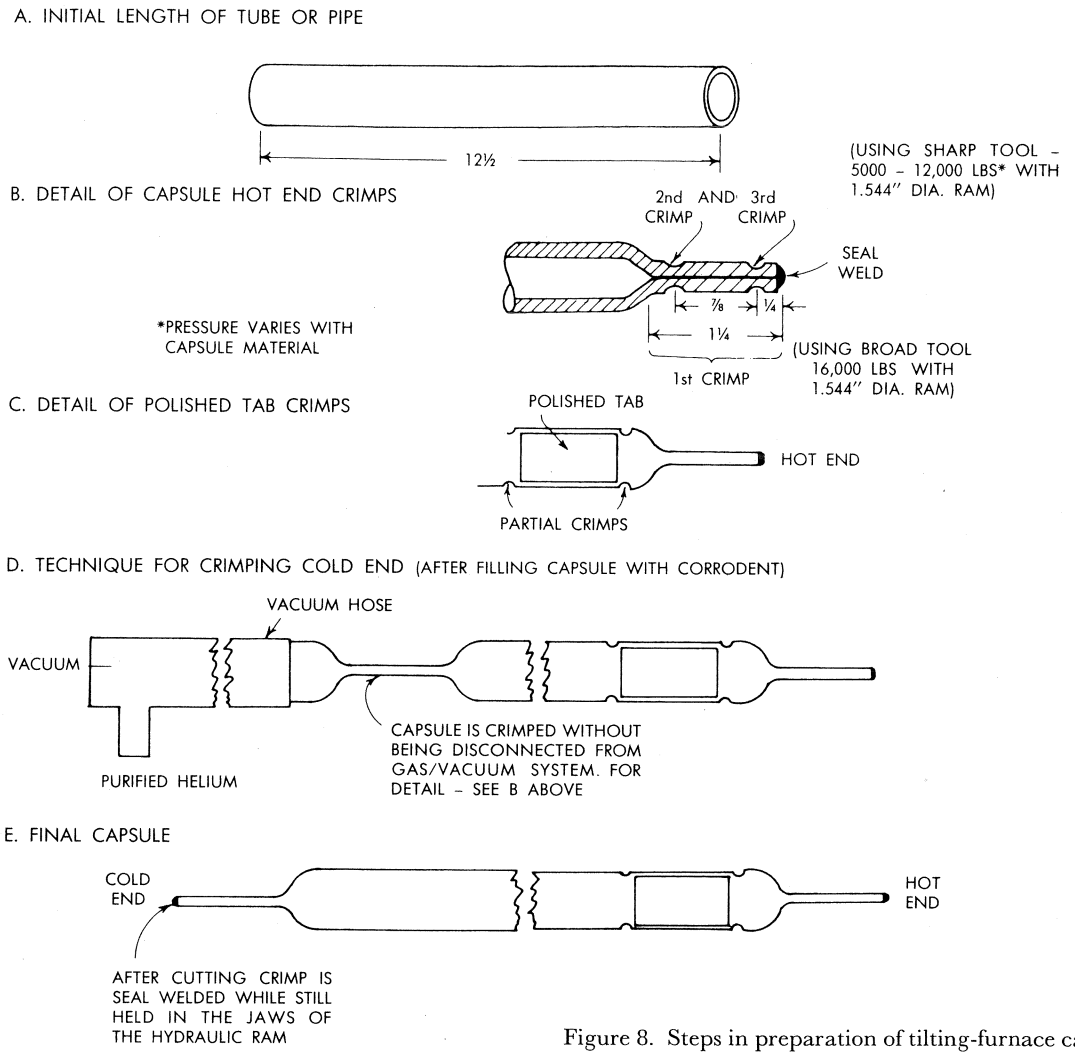

Figure 8. Steps in preparation of tilting-furnace capsule.

or 2500 hr in capsules made from fully annealed tubing or pipe. Test tabs were formed from the same stock and mounted in the hot end of the capsules. A group of two or four capsules was bundled together with two thermocouples and tested in a single furnace. The two thermocouple measuring junctions were located on the axis of the capsule bundle in contact with each capsule, as shown in Figure 7. One thermocouple measured and controlled the temperature at the hotter ends of the capsules, and the other measured the temperature at the colder ends.

With the particular capsule and furnace design used, it was found that the maximum temperature existed near the middle of the capsule rather than at the hot end where the test tab was located (see Appendix C). Corrosion product content of corrodent and corrosion product deposition could not, therefore, be principally associated with attack on test tabs. In spite of this limitation, the design was thought to be adequate for screening purposes.

A capsule was prepared as follows. A 12.5-in. length of pipe or tubing (Figure 8a) was sandblasted internally to remove any residual surface deposits. One end was then sealed by crimping in a hydraulic ram (Appendix D) followed by inert-arc fusion welding (Figure 8b). A test tab was then inserted into the tube and properly positioned and restrained in the sealed tube end by partial crimping (Figure 8c). After the first crimp was leak tested with a He mass spectrometer, the capsule was outgassed in a quartz tube at 550° to a pressure $<2\ \mu$ Hg.

The capsule was then transferred to a glass filling apparatus (Figure 9). The purified ternary

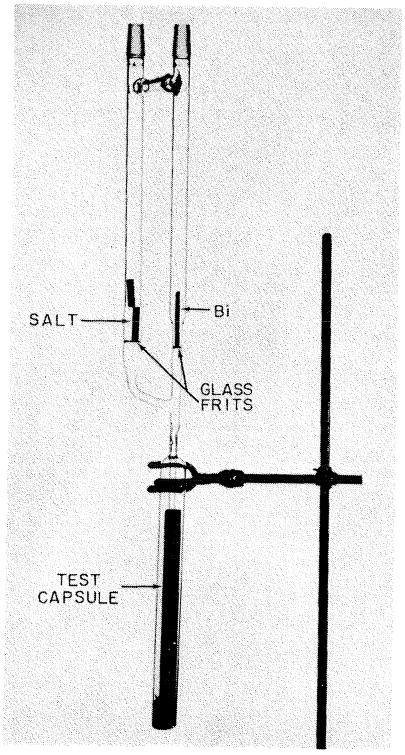

Figure 9. Apparatus in which tilting-furnace capsules were filled.

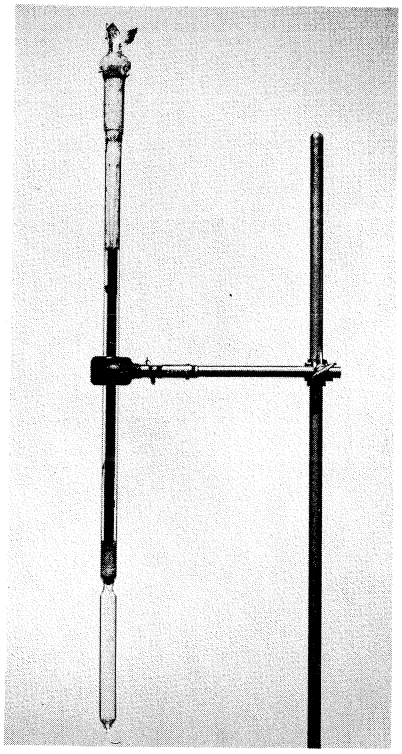

Figure 10. Glass-enclosed tilting-furnace capsule.

eutectic was charged into the left arm. For experiments involving both phases, Bi containing 1000 ppm U, 350 ppm Mg, and 350 ppm Zr was prepared by charging weighed quantities of Bi, U, Mg, and Zr into the right arm. In the single-phase experiments, just sufficient salt was used to immerse the test tab completely when it was in its lowest position in the tilting cycle. In the two-phase experiments, the test tab was again just fully immersed in this position with the Bi-salt interface at its center. The corrodents were vacuum-melted, and the fuel additives were dissolved by lightly vibrating the glass apparatus for about 2 hr. The corrodents were then filtered through Pyrex frits into the capsules below by use of Ar pressure. While the capsule was still blanketed with Ar, the lower section of the glass apparatus containing the capsule was sealed off.

Then, after the capsule cooled to room temperature, it was removed from the glass envelope, and its open end was quickly connected to a vacuum and purified He system. After the capsule was purged several times, it was filled with He to a pressure of 3 psig, and the open end was crimped (Figure 8d). While the tube was still held in the jaws of the hydraulic ram, its end was cut and seal-welded (Figure 8e). The integrity of this last seal-weld was checked by placing the capsule in a glass tube at 500°C and evacuating it to a mass spectrometer leak detector.

Most capsules were prepared as described above, but in certain cases it was necessary to modify the procedure. Mo, which is very brittle, and 1020 mild steel capsules, which had thick walls, could not be crimped, and both Mo and Ta, which are susceptible to air oxidation at high temperatures, had to be tested in the absence of air. The Mo and 1020 mild steel closures were made by inserting plugs into the capsule ends and then seal-welding them. The hot ends of the 1020 mild steel capsules were sealed in the open by inert-arc welding. After the capsule was filled, the second tube end (and both Mo tube ends) was seal-welded in a dry box. The atmosphere of Ar in the dry box had a dew point of −70°C.

The sealed Ta and Mo capsules were then enclosed in glass capsules under Ar in order to protect them from external air oxidation. Figure 10

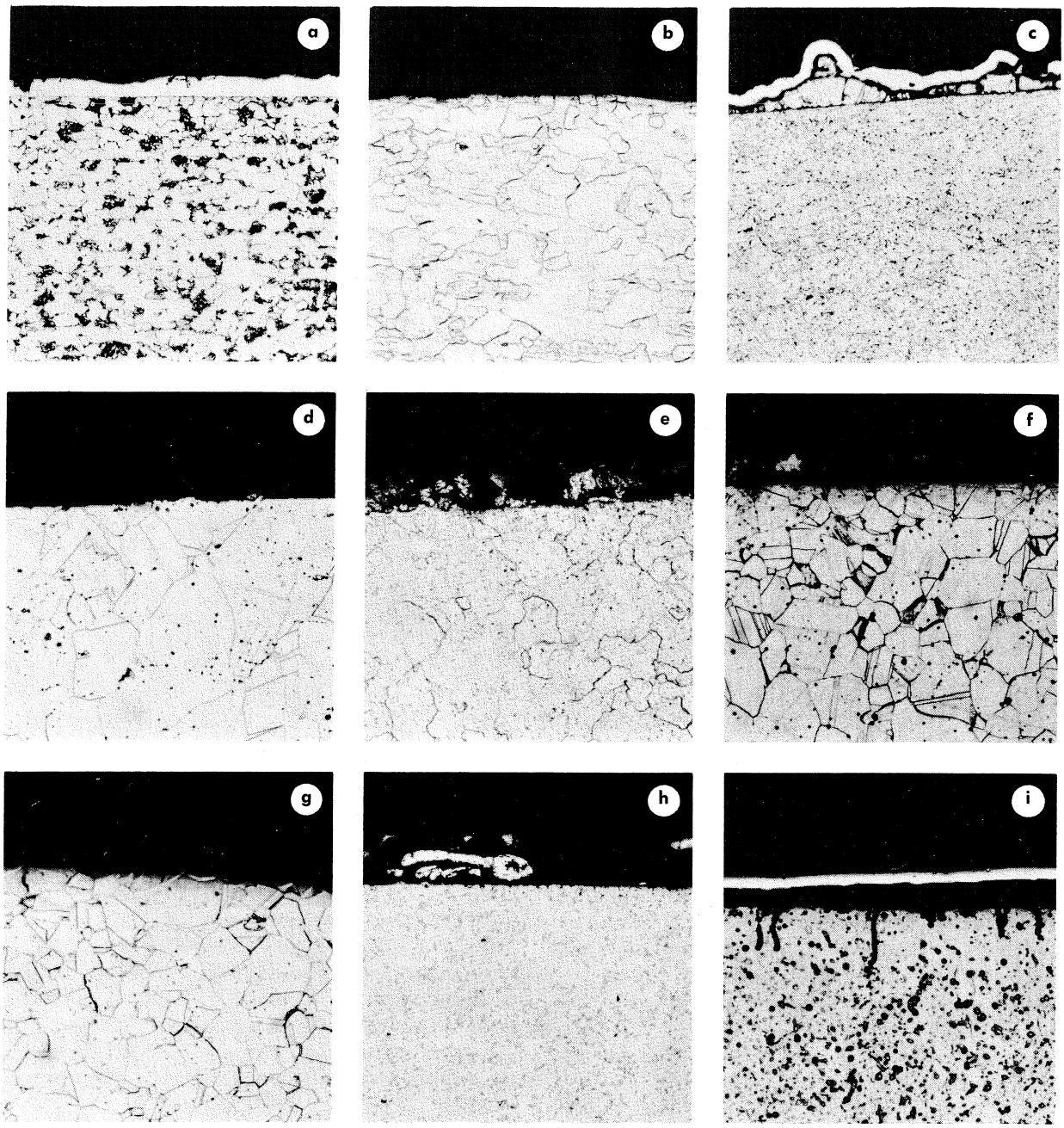

Figure 11. Photomicrographs (250×) of specimens exposed to NaCl-KCl-$MgCl_2$ in the tilting-furnace apparatus for 1000 hr (except as noted otherwise). Specimens were located in hot ends of capsules with hot end at 500°C and cold end at 450°C. Capsule designation is given in parentheses. (a) 1020 mild steel (T-12). Section through polished surface; nital etch. (b) Mo (K-12). Section through polished surface; etch: $K_3Fe(CN)_6$, KOH in H_2O. (c) 2¼ Cr – 1 Mo alloy steel (J-16). Section through cold end of polished side of specimen after 2500-hr exposure; nital etch. Note mass transfer deposit. (d) Inor-8 (P-13). Section through polished surface; aqua regia etch. (e) Type 410 stainless steel (E-13). Section through polished surface; etch: HCl, picric acid, alcohol. (f) Type 316 stainless steel (C-12). Section through polished surface; Marbles etch. (g) Inconel (G-13). Section through polished surface; etch: HCl, HNO_3. (h) Type 446 stainless steel (F-12). Section through polished surface; etch: HCl, picric acid, alcohol. (i) Ta (L-14). Section through polished surface; etch: HF, HNO_3.

Table 5

Results of Tilting-Furnace Screening Tests* Without $BiCl_3$

Test temperature difference: 50°C (500° – 450°)
Test duration: 1000 hr (except where noted)

Material	Corrodent: $NaCl-KCl-MgCl_2$ eutectic			Corrodent: Bi-U fuel/ternary eutectic		
	Type of corrosion on polished side	Maximum penetration, mils/yr	Weight change of tab, mg/cm²-yr	Type of corrosion on polished side	Maximum penetration, mils/yr	Weight change of tab, mg/cm²-yr
1020 Mild steel	None	0	−22	None	0	+3.3
2¼ Cr – 1 Mo steel	Intergranular and transgranular	3	+12.2	None	0	+3.8
2¼ Cr – 1 Mo steel**	None	0	32	None	0	+0.6
304 (ELC) S.S.	Intergranular	<0.4	−12.1	Intergranular and transgranular	15	−9.8
310 S.S.	None	0	− 2.8	Intergranular and transgranular	6.4	−102
316 S.S.	Intergranular	<0.4	− 2.9	Intergranular	6.0	−7.1
347 S.S.	Intergranular and transgranular	4.7	− 4.6	"	10	−7.2
410 S.S.	Intergranular	1.0	− 4.1	"	6	−57
430 S.S.	Transgranular	2	− 0.8	"	5.2	Not measured
16-1 Croloy	Intergranular	<0.4	+10.7	"	4.4	−40
446 S.S.	Intergranular	<0.4	+ 4.2	None	0	−3
Inconel	Intergranular	1.8	− 3.2	Intergranular and transgranular	Too extensive to measure	−525
Hastelloy C	Not tested			Intergranular and transgranular	32	−162
Inor-8	Transgranular	2	Not measured	Intergranular and transgranular	Too extensive to measure	−1000
Molybdenum	None	0	− 2.8	None	0	+0.4
Tantalum	Intergranular	2.9	− 1.0	Transgranular	4.1	−8.3

*Results are averages of 2 tests.
**Test duration = 2500 hr.

Table 6

Results of Tilting-Furnace Screening Tests* (Welded Tabs)

Test temperature differences: 50°C (500°–450°)
Test duration: 2500 hr
Corrodent: $NaCl-KCl-MgCl_2$ eutectic

Material	Polished side of tab			Weld	
	Type of corrosion	Max. penetration, mils/yr	Weight change of tab, mg/cm²-yr	Type of corrosion	Max. penetration, mils/yr
2¼ Cr – 1 Mo steel	Transgranular	<0.15	+34.0	Intergranular and transgranular	<0.15
347 S.S.	"	0.7	− 1.2	Transgranular	0.2
446 S.S.	"	0.25	−14	Intergranular and transgranular	<0.15
Inconel	"	0.5	+ 0.16	Transgranular	0.7

*Results are averages of 2 tests. Welds were stress relieved.

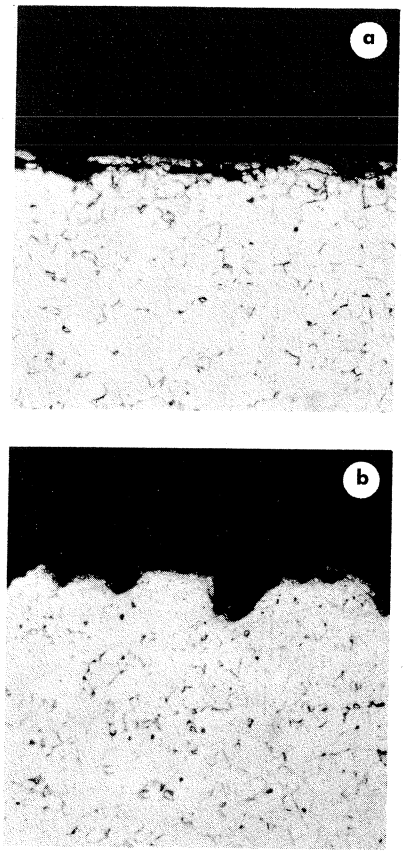

Figure 12. Photomicrographs (250×) of specimen of type 347 stainless steel (capsule D-12) exposed to NaCl-KCl-$MgCl_2$ eutectic for 1000 hr in the tilting-furnace apparatus. Specimen located in hot end of capsule with hot end at 500°C and cold end at 450°C. Marbles etch. (a) Section through polished surface. (b) Section through sand-blasted surface.

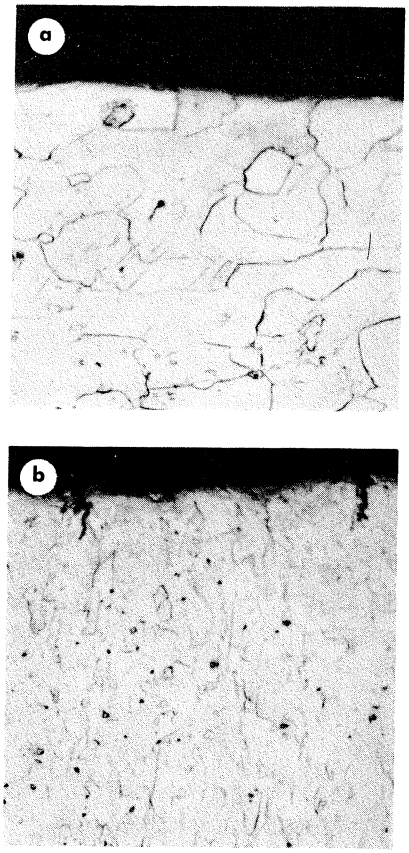

Figure 13. Photomicrographs (250×) of Ta (capsule L-19) exposed to NaCl-KCl-$MgCl_2$ eutectic for 1000 hr in the tilting-furnace apparatus. Polished specimen located in hot end of apparatus with hot end at 500°C and cold end at 450°C. Etch: HF, NH_4F. (a) Section through polished specimen surface. (b) Section through inner surface of capsule wall.

shows a typical glass-enclosed Mo capsule. Four glass-to-metal seals for thermocouple leads are located at the upper end of the glass envelope.

The procedure followed for preparing those metallic capsules which contained $BiCl_3$ was identical to that described above except that in all cases both the $BiCl_3$ additions and the final closures were made in the dry box.

The filling procedure for the glass capsules containing long Au tabs running their entire length was considerably simplified. The purified salt was charged into the glass filling apparatus, vacuum-melted, and filtered with He pressure into the glass test capsule containing the test tab and $BiCl_3$. While still under the He blanket, the glass capsule was sealed off. In these runs, the $BiCl_3$ was not added in a dry box, but the weighings and additions were done as rapidly as possible to minimize exposure to air.

All corrodent combinations except LiCl-KCl eutectic were used in the tilting-furnace tests. Typical photomicrographs showing a specimen from each group of similar materials (e.g., 300 series stainless steels, 400 series stainless steels, etc.) are shown in Figures 11 to 18. Data for individual capsules including corrodent chemical analyses are given in Appendix E. The results follow.

NaCl-KCl-$MgCl_2$ Eutectic Tests

Type 310 stainless steel, 1020 mild steel (Figure 11a), and Mo (Figure 11b) were not attacked after 1000-hr exposure to eutectic salt (Table 5). No corrosion was found in a 2500-hr test of 2¼ Cr – 1 Mo steel (Figure 11c). Slight intergranular

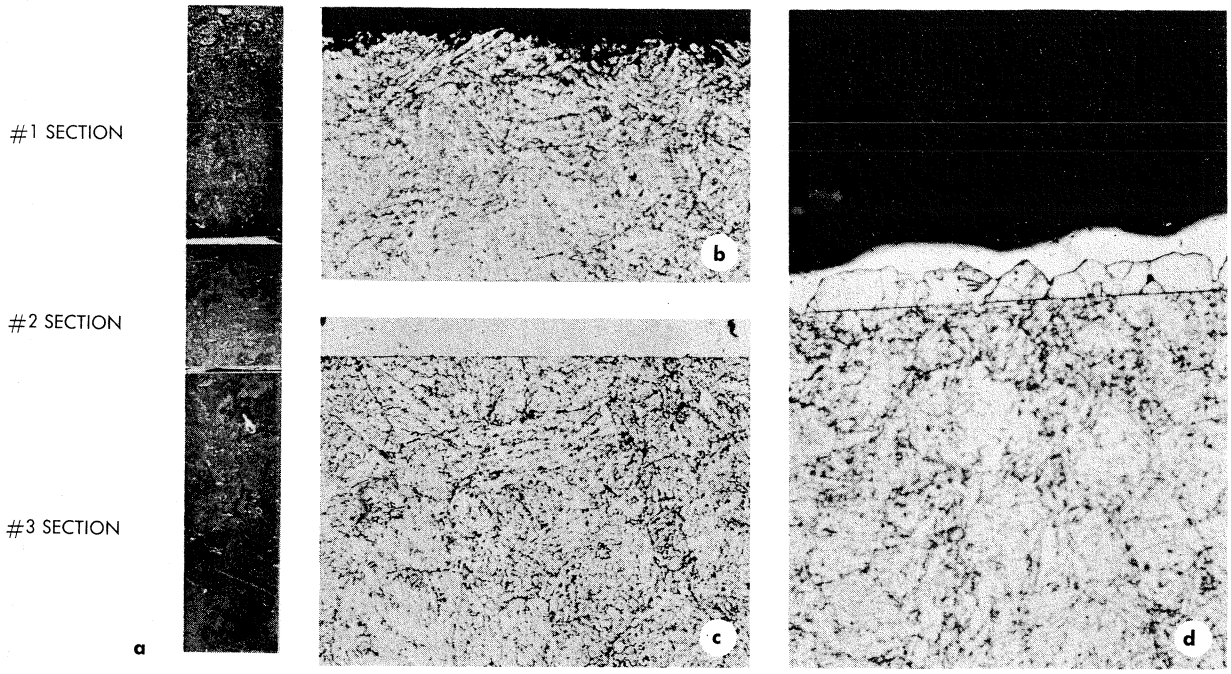

Figure 14. 2¼ Cr – 1 Mo alloy steel specimen (capsule J-12) exposed to NaCl-KCl-$MgCl_2$ eutectic for 1000 hr in the tilting-furnace apparatus. Specimen located in hot end of capsule with hot end at 500°C and cold end at 450°C. Nital etch. (a) Photograph of assembled specimen. Photomicrographs (250×): (b) Section through polished surface at hot end (#3 section). (c) Section through polished surface of central portion (#2 section). (d) Section through polished surface of cold end (#1 section).

corrosion of most of the other materials was found. Type 347 stainless steel (Figure 12a) and 2¼ Cr – 1 Mo steel (1000-hr test) were attacked transgranularly also. Inor-8 (Figure 11d) and type 430 stainless steel showed slight transgranular attack only. Traces of magnetic deposition were present in the cold ends of several capsules, but in amounts too small for analysis.

Figures 12a and 12b illustrate the difference in the attack found on sandblasted and mechanically polished surfaces of a single tab. Figures 13a and 13b illustrate the results obtained in two of the 1000-hr exposures of Ta to the ternary salt, when no attack was found on the test tab, but intergranular corrosion was found on the capsule wall. Evidence for mass transfer from one end of a test tab to the other was found in one 2¼ Cr – 1 Mo, 1000-hr test (Figure 14). A photograph of the assembled tab is shown in Figure 14a. Attack is indicated at the hotter end (Figure 14b); no attack is seen in the central portion (Figure 14c); and deposition of material (which was magnetic) is found at the colder end (Figure 14d).

Similar results (Table 6) were obtained when stress-relieved weld specimens of 2¼ Cr – 1 Mo steel, types 347 and 446 stainless steel, and Inconel were tested for 2500 hr (Figure 15). Negligible corrosion was observed at each weld.

Chemical analyses (see Appendix E) of the corrodents from the steel and Ni alloy capsules showed that Cr was present in the largest concentration (75 to >1000 ppm), followed by Fe (20 to 190 ppm) and Mn (20 to 320 ppm). Very little Ni (40 ppm maximum) was found. Up to 100 ppm Ta and 600 ppm Mo were found in their respective tests.

Bi-U Fuel/Ternary Eutectic Tests

Mo, 1020 mild steel, 2¼ Cr – 1 Mo steel, and type 446 stainless steel were not attacked after 1000-hr exposures to Bi-U/ternary salt (Table 5 and Figures 16a, b, c). No corrosion was found after a 2500-hr test of 2¼ Cr – 1 Mo steel (Figure 16d).

Ta (Figure 16e) was transgranularly attacked. Previous tests at Ames Laboratory[8] with Bi alone did not produce any significant attack at 1000°C.

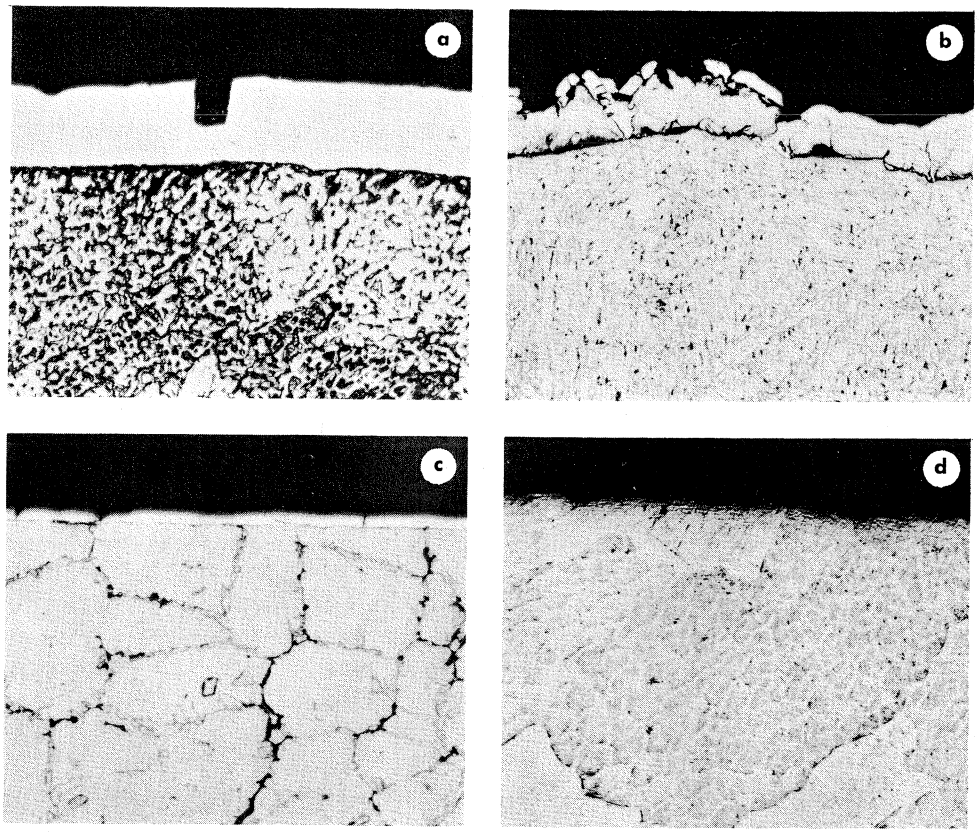

Figure 15. Photomicrographs (250×) of fusion-welded specimens exposed to NaCl-KCl-$MgCl_2$ eutectic for 1000 hr in the tilting-furnace apparatus. Specimens located in hot ends of capsules with hot end at 500°C and cold end at 450°C. (a) Section through surface of type 347 stainless steel weld (capsule D-20); Marbles etch. (b) Section through surface of 2¼ Cr – 1 Mo alloy steel weld (capsule J-23); nital etch. (c) Section through surface of type 446 stainless steel weld (capsule F-18); picric acid etch. (d) Section through surface of Inconel weld (capsule G-14); picric acid etch.

Type 446 (Figure 16c) was the only 400 series stainless steel that was not attacked. The corrosion resistance of type 430 stainless steel was like that of 16-1 Croloy [similar to type 431 (ELC) stainless steel]. Type 410 stainless steel (Figure 16f) was the least resistant in this series.

Figures 16g, h, and i show the appearance of type 347 stainless steel specimens as a function of surface treatment: mechanical polishing, electropolishing, and sandblasting.

Corrosion of the other materials was primarily intergranular. In most cases corrosion was accompanied by metallic deposition at the cold end, the deposition generally being greater with greater tab weight loss. The capsule and tab surfaces were generally found to be wetted by the Bi. No salt was found at the Bi – capsule wall interface, which indicates that the salt may not creep into the Bi fuel system in a processing plant.

The corrosion occurring in the tilting-furnace tests with Bi-U/ternary salt corrodents was similar in type and extent to that caused by Bi-U fuel in the absence of salt. Alloys containing Ni suffered severe attack, accompanied by significant weight losses and extensive mass transfer (Figures16j, k). Ni is soluble in Bi, and the corrosion was generally by intergranular attack. In the cases of types 304 (ELC) and 310 stainless steel and the high Ni alloys (Inconel, Inor-8, and Hastelloy C, this dissolution was so great that extensive transgranular attack also occurred.

Fe and Ni were the principal corrosion products found upon analysis of the corrodents from steel and Ni alloy capsules (see Appendix E). The Ni

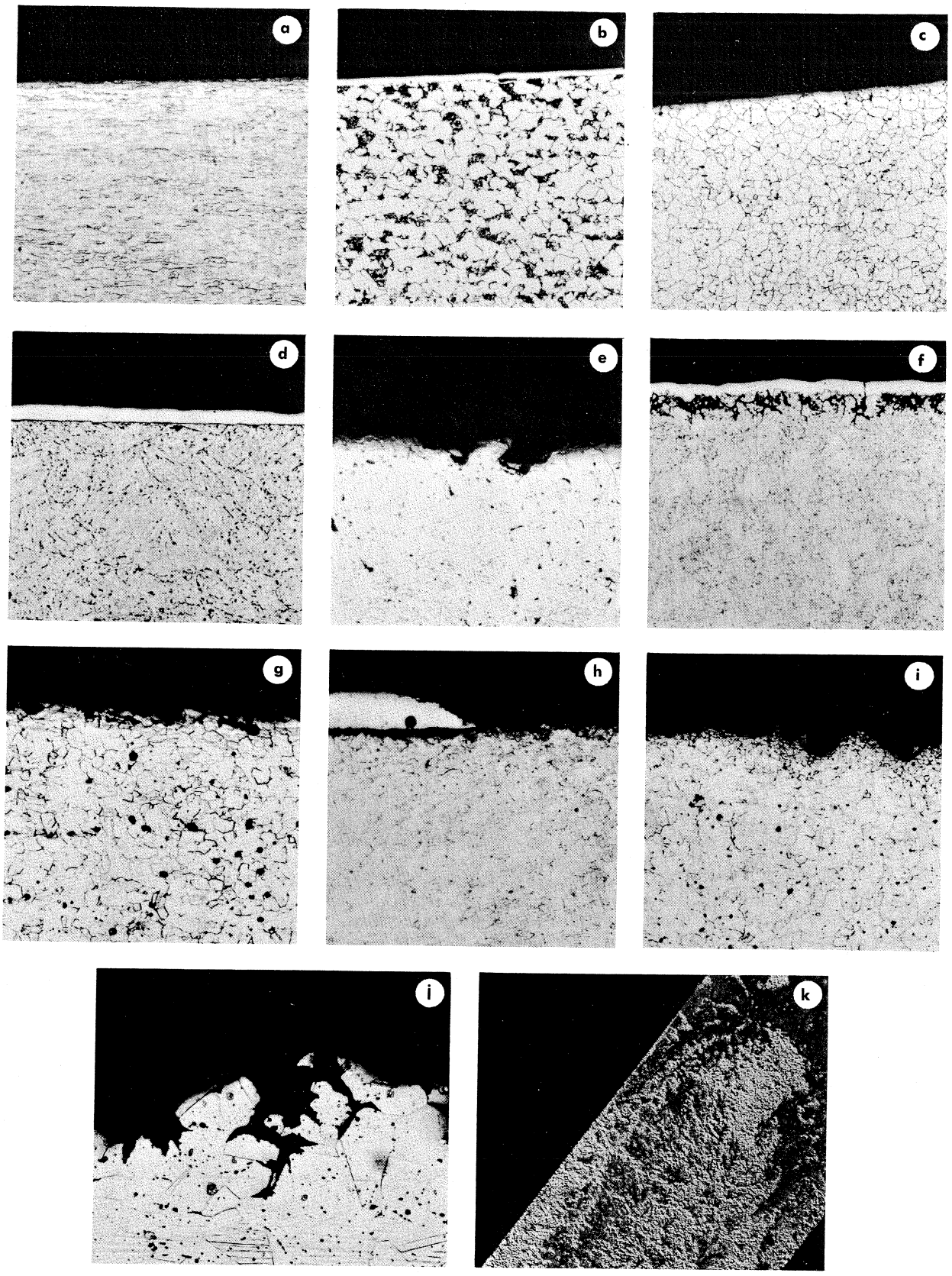

Figure 16. Photomicrographs (250×) of specimens exposed to NaCl-KCl-$MgCl_2$ and Bi-U fuel in the tilting-furnace apparatus for 1000 hr (except as noted otherwise). Capsule designation is given in parentheses. (a) Mo (K-11). Section through polished surface; etch: $K_3Fe(CN)_6$, KOH in H_2O. (b) 1020 mild steel (T-10). Section through polished surface; nital etch. (c) Type 446 stainless steel (F-10). Section through polished surface; etch: modified Carapella's reagent. (d) 2¼ Cr – 1 Mo alloy steel (J-15); 2500-hr exposure. Section through polished side of tab; nital etch. (e) Ta (L-12). Section through polished side of tab; etch: HF, HNO_3. (f) Type 410 stainless steel (E-11). Section through polished side of tab; etch: HCl, picric acid, alcohol. (g) Type 347 stainless steel (D-10). Section through polished side of tab; Marbles etch. (h) Type 347 stainless steel (D-13). Section through electropolished tab; Marbles etch. (i) Type 347 stainless steel (D-10). Section through sandblasted side of tab; Marbles etch. (j) Inor-8 (P-10). Section through polished side of tab; aqua regia etch. (k) Hastelloy C (H-11). Section through polished side of tab, 2.5×.

concentrated principally in the Bi phase (up to 1.65%), while Fe was found primarily in the salt (up to 575 ppm). No Mo was found in the Bi and <100 ppm in the salt, while 30 ppm Ta was found in the Bi and 45 ppm in the salt.

Ternary Eutectic/$BiCl_3$ and Bi-U Fuel/Ternary Eutectic/$BiCl_3$ Tests

Mo and Ta were tested with a 4.76% solution of $BiCl_3$ in ternary eutectic alone and in the presence of Bi-U fuel. Au was tested with a 4.76% solution of $BiCl_3$ in ternary eutectic alone. Because of experimental difficulties, not all the tests were of the same duration. The Mo and Ta were only slightly pitted or corroded transgranularly, although the $BiCl_3$ was almost completely reduced. Only Au did not corrode significantly or reduce $BiCl_3$ during these tests. See Figures 17 and 18 and Table 7 for details.

THERMAL CONVECTION LOOP TESTS

Mass transfer corrosion tests were performed in six thermal convection loops made of types 347 and 410 stainless steel and 2¼ Cr – 1 Mo steel. Besides being larger than tilting-furnace capsules, these loops have the advantage that they may be sampled during the course of an experiment. Salt velocities comparable to those expected in a processing plant (0.2 to 0.3 ft/sec) may be obtained.

All loops except F and L-1 were fabricated in the shape shown in Figure 19 from a 40-in. length of ½-in. pipe. An 8-in. length of 4-in. pipe was placed at the top of the harp to serve as a surge tank. Loops F and L-1 were made from 72-in. lengths of ½-in. pipe bent in a semicircular shape at the bottom. The surge tanks were made from 7-in. lengths of 3- and 4-in. pipe, respectively. A 5-in. test section was inserted in the upper portion of the hot leg. The test section, originally 6 in. long, was machined and polished on the inside. The dimensions of the section were recorded, and a 1-in. length was removed for use as a standard for comparison at the end of the run. An air lock with a sliding Teflon compression seal assembly and a 1½-in. ball valve was mounted on the surge tank. This chamber provided a means of taking samples from the loop during operation. Prior to construction, all materials were sandblasted except that in Loops F and L-1, which was electropolished. After fabrication, each loop was thoroughly cleaned with acetone and alcohol to remove moisture and grease. In addition, Loop L-7, which was constructed of 2¼ Cr – 1 Mo steel, was hydrogen-fired to remove oxides and moisture from the pipe walls. Hydrogen flow was stopped when a dew point of −40°C was obtained at an average loop temperature of 550°C. The loop was then purged with He.

A He mass spectrometer leak test was performed on each loop and its associated gas and

Table 7

Results of Tilting-Furnace Screening Tests* With $BiCl_3$

Test temperature difference: 50°C (500°–450°)

Material	Length of test, hr	Type of corrosion on polished side of tab	Maximum penetration, mils/yr	Weight change of tab, mg/cm²-yr	Residual % $BiCl_3$ in salt
	Corrodent: NaCl-KCl-$MgCl_2$ eutectic plus 4.76% $BiCl_3$				
Molybdenum	600	Pitting	2.2	Not measured	<0.05
Tantalum	1600	Pitting	1.4	−45	<0.05
Gold	1000	Intergranular	1.0	− 1.1	4.92
	Corrodent: Bi-U fuel/ternary eutectic plus 4.76% $BiCl_3$				
Molybdenum	2500	Transgranular	1.8	− 1.1	0.24
Tantalum	2500	Transgranular	1.8	− 7.9	0.15

*Results are averages of 2 tests.

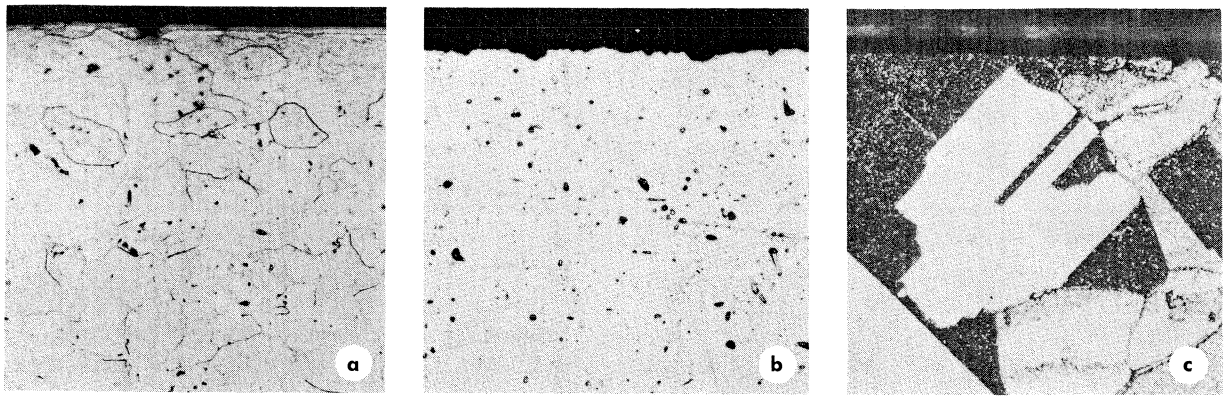

Figure 17. Photomicrographs (250×) of tabs exposed to NaCl-KCl-$MgCl_2$ eutectic containing 5% $BiCl_3$ in the tilting-furnace apparatus. (a) Mo (capsule K-17). Section through polished side of tab; 600-hr exposure; etch: $K_3Fe(CN)_6$, NaOH in H_2O. (b) Ta (capsule L-23). Tab cleaned prior to exposure by degreasing only; 1600-hr exposure; etch: HF, NH_4F. (c) Au (capsule Au-1). Hot end of tab running full length of (glass) capsule; 1000-hr exposure; aqua regia etch.

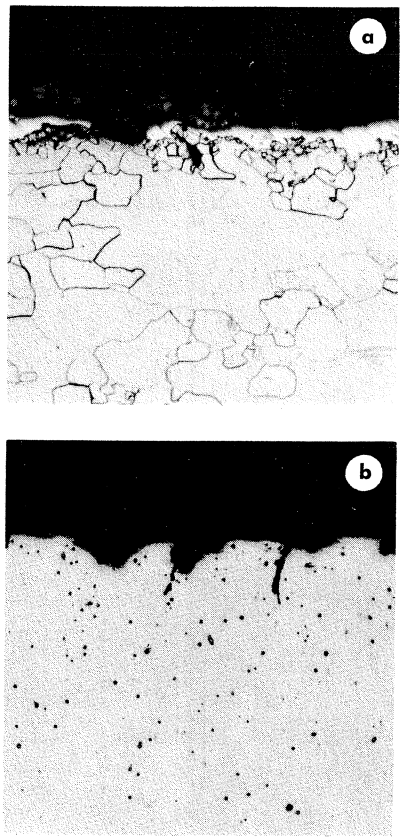

Figure 18. Photomicrographs (250×) of tabs exposed to Bi-U fuel and NaCl-KCl-$MgCl_2$ eutectic containing 5% $BiCl_3$ for 2500 hr in the tilting-furnace apparatus. (a) Mo (capsule K-14). Section through polished side of tab; etch: $K_3Fe(CN)_6$, NaOH in H_2O. (b) Ta (capsule L-20). Tab cleaned prior to exposure by degreasing only; no etch.

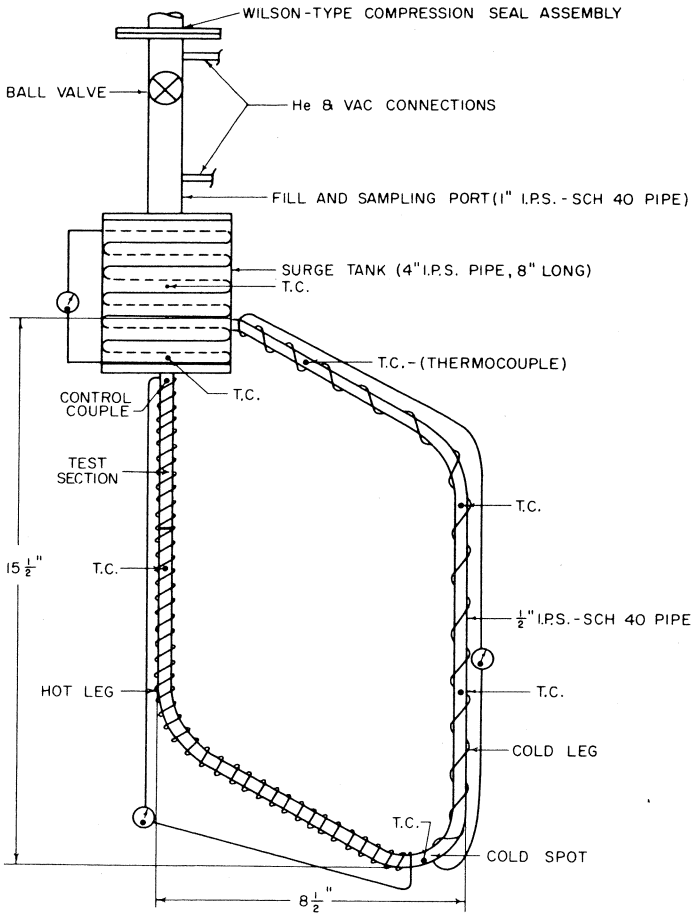

Figure 19. Schematic diagram of typical ternary salt thermal convection loop showing heater circuit windings and thermocouple measuring junction locations.

vacuum piping before the installation of electric heating elements.

Three circuits of 20 gauge nichrome heater wire were used to heat each loop. The hot leg was wound with 25.2 ft of wire in closely spaced turns and the surge tank with 23.3 ft of wire. A 1-in. space containing no heater wire provided a cold spot on the cold leg. The 15-ft length of wire used on the remainder of the cold leg was applied in widely spaced turns. Loops F and L-1 were each wrapped with 41 ft of wire on the hot legs, 8 ft on the cold legs, and three 200-w strip heaters on the surge tank.

Eight thermocouples were used to determine pipe surface temperatures on each loop; 18 were used on Loops F and L-1. The maximum loop temperature was monitored by a thermocouple located on the hot leg just below the surge tank, and the minimum by one at the cold spot. The other thermocouples were placed around the rest of the loop.

All portions of the loop were insulated with 2½ in. of Owens-Corning Kaylo. A separate block of insulation was used on the cold leg to permit easy removal during operation.

Each loop was degassed before charging with salt by heating under vacuum at a rate such that the pressure remained below 5 μ Hg. A final pressure of <1 μ Hg was obtained at 550°C. The temperature was then lowered to 500°C and the loop pressurized to 5 psig with He.

Each ternary salt loop was charged with 2550 g of the eutectic. The salt was introduced into a loop by inserting a salt-filled glass tube (open at

Table 8

Results of Thermal Convection and Forced Convection Loop Corrosion Tests

	Corrodent: LiCl-KCl Eutectic Thermal convection loops		
	Loop F	Loop L-1	Loop L-3
Material	347 S.S.	410 S.S.	2¼ Cr – 1 Mo
Operating time, hr	5500	2200	697
Max. salt temperature, °C	575	570	550
Salt ΔT, °C	155	160	150
Calculated velocity, ft/sec	0.68	0.75	0.48
Type of corrosion	Intergranular	Transgranular	*
Max. attack, mils/yr	0.5	2.1	*
Composition of deposited material	None	62% Fe – 38% Cr	*

	Corrodent: $NaCl-KCl-MgCl_2$ Eutectic				
	Thermal convection loops			Forced circulation loop	
	Loop L-5	Loop L-6	Loop L-7	Loop M	
Material	347 S.S.	410 S.S.	2¼ Cr – 1 Mo	347 S.S.	
Operating time, hr	2467	3971	6281	1034	656
Max. salt temperature, °C	500	494	501	520	515
Salt ΔT, °C	45	42	49	Isothermal	Isothermal
Calculated velocity, ft/sec	0.25	0.24	0.26	13.2	1.8-7.9
Type of corrosion	Intergranular	Transgranular	Transgranular and intergranular	Transgranular	Transgranular
Max. attack, mils/yr	3.9	3.3	3.1	1.3	10.7**
Composition of deposited material	Fe-Cr, 2% Ni	Fe – 10% Cr†	Fe – 2% Cr	—	—

*The loop could not be examined metallurgically because the pipe ruptured after accidental overheating.
**Pipe specimen surface was sandblasted prior to the test. All others in the table were mechanically polished.
†Loop plugged.

the bottom) at room temperature into the air lock on the top of the loop. After purging of the lock with He, the inverted glass tube was lowered into the heated surge tank where the salt melted and flowed out of the tube.

The binary salt loops were charged from a portable stainless steel melt tank through a flanged connection on the surge tank. LiCl and KCl were charged into the tank, dried, and melted under high vacuum. The molten eutectic was transferred by application of He pressure to the tank. Oxide impurities were removed by a porous 20-μ stainless steel filter located in the transfer line.

He, purified by passage through a silica gel drier and tubes of Ti chips held at 825° to 850°C, was used as the cover gas for each loop.

Accurate temperature control was imperative during operation of the loops. Three separate transformers, one for each heater circuit, were used.

After loading, loop temperatures were stabilized at 500°C. Insulation was then removed from the cold leg. The hot leg temperature of each loop was controlled, and the cold leg and surge tank heaters were adjusted to give the desired temperature difference.

A flexible thermocouple probe was inserted through the sliding Teflon compression seal into the air lock. After purging with He, the probe was inserted into the salt stream to obtain a bulk temperature profile of the loop. The bulk temperature of the hot leg was $\approx$2°C lower than the adjacent pipe surface temperature. The surface temperature in the cold leg was $\approx$20°C below the corresponding bulk temperature.

Salt velocities obtained for any temperature difference were calculated from the following formula:

$$V = \left[\frac{\Delta h(\rho_c - \rho_h) gD}{4fL\rho_{av}} \right]^{1/2}$$

where

V = salt velocity, ft/sec;
Δh = difference in height between points of maximum and minimum loop temperature, ft;
$\rho_h, \rho_c, \rho_{av}$ = salt densities[9] at maximum, minimum, and average temperature, lb/ft^3;
g = gravitational constant, ft/sec^2;
D = pipe diameter, ft;
L = equivalent length of pipe, ft; and
f = Fanning friction factor.

The ternary salt was generally sampled weekly with degassed graphite cups by the thief method[10] and analyzed for Fe, Cr, Mn, and Ni. The binary salt loops were sampled only infrequently.

A radiograph of each ternary salt loop was taken weekly to observe corrosion and deposition changes. A 700 to 900-mC Ir^{192} source was used.

The results are shown in Table 8 and Appendix F and described below.

Loop F

This type 347 stainless steel, binary salt, thermal convection loop was shut down voluntarily after 5500 hr of operation at a surface temperature difference of 155°C and a maximum hot leg surface temperature of 575°C. The calculated velocity through the loop was 0.68 ft/sec.

Metallurgical examination of the loop showed no plugging of the cold leg and a maximum intergranular corrosion of the hot leg of $\approx$0.3 mil.

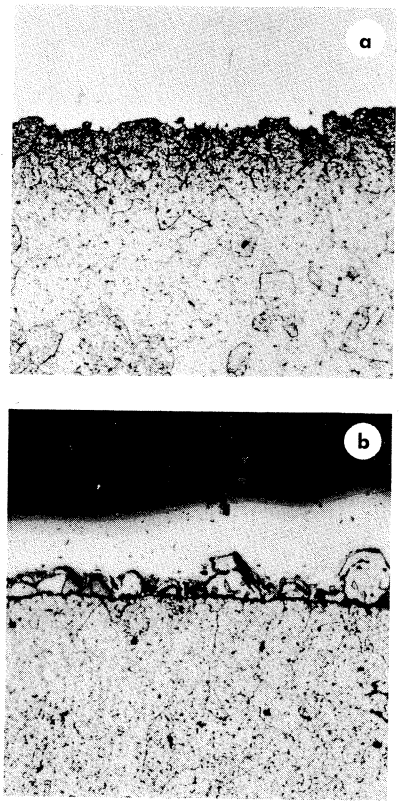

Figure 20. Photomicrographs (250×) of portions of thermal convection Loop L-1 (type 410 stainless steel). HCl, picric acid, alcohol etch. (a) Hot leg test specimen showing intergranular attack. (b) Cold leg showing deposition of Fe-Cr particles.

Loop L-1

This type 410 stainless steel, binary salt, thermal convection loop was operated for 2200 hr at a surface temperature difference of 160°C and a maximum surface temperature of 570°C. The calculated velocity through the loop was 0.75 ft/sec. The loop was shut down because during start-up after a power failure melting of the salt produced a rupture in the wall of the hot leg.

Samples taken for corrosion product analysis during loop operation showed that the Fe concentration rose to 150 ppm and Mn and Cr remained constant at 65 and 115 ppm respectively. Ni was not detected (limit of detection 10 ppm). Salt samples taken from various parts of the loop after shutdown showed that the Fe concentration varied between 85 and 290 ppm, whereas the Mn and Cr concentrations were uniform at 50 and 10 ppm, respectively.

Metallographic examination of the loop showed the presence of considerable transgranular corrosion of the hot leg (0.5 mil deep; see Figure 20a), and the start of an Fe-Cr plug in the cold leg (Figure 20b) analyzed as 62% Fe and 38% Cr. Although the loop was shut down because of a mechanical mishap, it would have been only a short time before the cold leg deposition plugged the pipe. On the basis of this experiment, the use of type 410 stainless steel appears to be unsatisfactory for LiCl-KCl eutectic service.

Loop L-3

This 2¼ Cr – 1 Mo steel, binary salt, thermal convection loop was operated with a surface temperature difference of 150°C and a hot leg surface temperature of 550°C. The loop was shut down after 697 hr of operation at a calculated velocity of 0.48 ft/sec when the hot leg temperature had risen sharply because the temperature controller failed to function. In the attempt to restart the loop, the pipe wall was ruptured as a result of uneven expansion of the salt. Because of the rupture, metallurgical examination of the loop was impossible. Radiographic inspection indicated a plug in the cold spot of the loop.

Only one sample was obtained during loop operation. After 210 hr of operation, chemical analysis showed the following concentrations of corrosion products: Fe, 1100 ppm; Mn, 95 ppm; Cr, 20 ppm; and Mo, maximum 50 ppm.

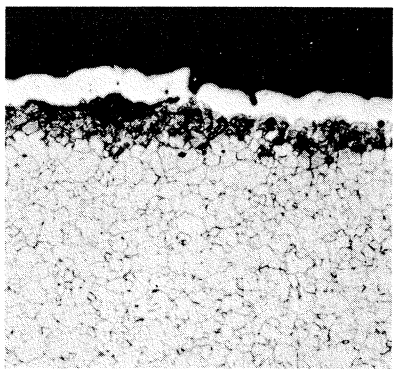

Figure 21. Photomicrograph (250×) of portion of hot leg from thermal convection Loop L-5 (type 347 stainless steel) showing intergranular corrosion. Marbles etch.

Loop L-5

This type 347 stainless steel, ternary salt, thermal convection loop was operated for 2467 hr with maximum bulk temperatures of 500° and 504°C. The corresponding bulk temperature differences of 41° and 54°C were maintained for 1030 and 1344 hr, respectively. Velocities through the loop were 0.22 and 0.27 ft/sec, respectively.

The loop operated satisfactorily until a graphite sampling cup was accidentally dropped into the surge tank, causing the temperature difference to increase to 69°C with a maximum temperature of 524°C. After 93 hr of operation at this temperature, the loop was shut down. Radiographic inspection during operation and after shutdown indicated no apparent corrosion in the hot leg and no deposition in the cold leg.

The results of the chemical analysis for corrosion products in salt samples taken twice weekly are as follows: After an initial increase to 50 ppm within the first 100 hr, the Cr concentration increased at a constant rate to 375 ppm at the conclusion of the test. The Mn concentration increased to 25 ppm at 1300 hr and thereafter remained constant. Ni was not detected (limit of detection 10 ppm). The Fe concentration was erratic, reaching values as high as 300 ppm.

Metallographic examination of the loop showed the presence of a very small amount of intergranular corrosion (<1 mil deep) in the hot leg (Figure 21), whereas none was observed on the machined standard hot test specimen. Slight deposition was observed in the cold leg. The deposit was removed and identified by spectrographic analysis as an Fe-Cr alloy containing ≈2% Ni.

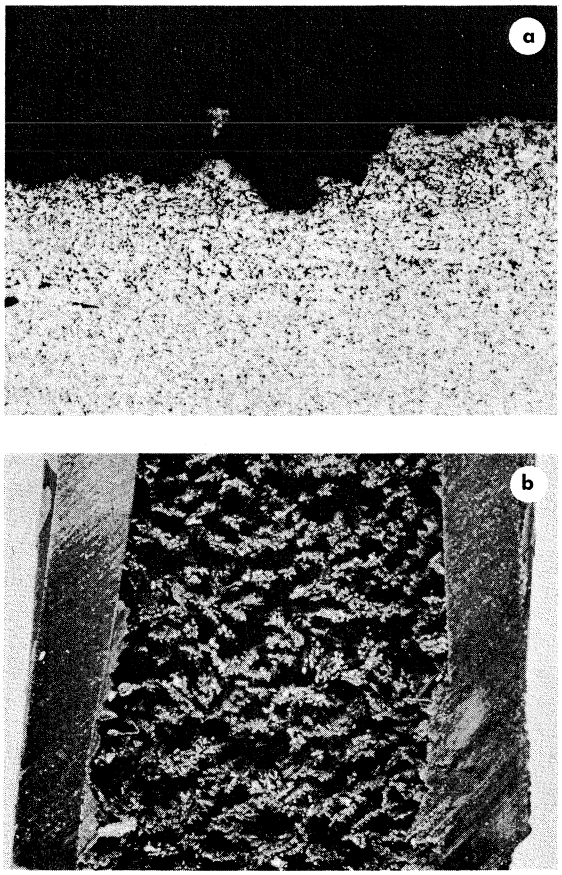

Figure 22. Photomicrographs of portion of thermal convection Loop L-6 (type 410 stainless steel). (a) Hot leg, showing transgranular corrosion; HCl, picric acid, alcohol etch (250×). (b) Dense Fe – 10% Cr deposit in cold leg (3×).

Loop L-6

This type 410 stainless steel, ternary salt, thermal convection loop was shut down after 3971 hr of operation at a bulk temperature difference of 42°C and a maximum bulk temperature of 494°C. The maximum velocity through the loop was 0.24 ft/sec. Radiographic inspection of the loop indicated no corrosion in the hot leg and some deposition in the cold leg. The deposition was first detected after 1400 hr and increased steadily throughout the remainder of the run. The loop was shut down when the deposition restricted the salt flow so that the cold leg froze and the hot leg reached a maximum temperature of 550°C.

Corrosion product concentrations in the salt were as follows: The Fe content increased from 10 to 700 ppm in the first 1400 hr and then remained constant until 3000 hr. At that time, an unexplained decrease to 450 ppm occurred, and the concentrations remained constant until shutdown. The Cr content increased at a constant rate to a value >1000 ppm. Mn increased to 80 ppm, and Ni was not detected (limit of detection 10 ppm).

Metallographic inspection of the loop revealed a slight amount of transgranular corrosion in a small area of the hot leg (Figure 22a), the maximum attack being $\approx$1.5 mils. Welds appeared to be unaffected by the salt. Deposition was found at the bottom of the cold leg extending over an area of $\approx$3 in.^{2} (Figure 22b). Chemical analysis showed that this material consisted of a dense Fe-Cr alloy containing 10% Cr. Study of the surge tank wall indicated no direct attack; however, the area below the salt level appeared to be free of any scale, whereas above this level scale was evident. At the salt-to-He interface, a ¼-in. ridge of Fe-Cr alloy was found adhering to the wall of the tank, which had the same general structure as the other plug material found in the loop.

Loop L-7

This 2¼ Cr – 1 Mo steel, ternary salt, thermal convection loop was operated for 6281 hr before it was shut down voluntarily. Bulk temperature differences of 57° and 49°C with maximum bulk temperatures of 511° and 501°C were maintained for 545 and 5736 hr, respectively. Calculated velocities through the loop were 0.33 ft/sec for 545 hr and 0.26 ft/sec for 5736 hr. Prior to start-up, the loop was cleaned by hydrogen-firing at 550°C in addition to sandblasting as in Loops L-5 and L-6. Radiographic inspection during operation and after shutdown indicated no apparent corrosion in the hot leg and steadily increasing deposition in the cold leg after 2600 hr of operation.

The results of the corrosion product analysis are as follows. The Fe concentration increased in stepwise fashion: it went from 10 to 1440 ppm in the first 2100 hr of operation, remaining at 1440 ppm up to 4100 hr; it increased to 1750 ppm by 4550 hr, remaining at this value up to 5900 hr; and it increased finally to 2100 ppm, where it remained until shutdown. Cr, which was not detected for the first 700 hr, increased to 210 ppm after 2700 hr of operation; it then increased rapidly to 580 ppm, where it remained constant until 3600 hr, at which point it decreased unexplainably to 400 ppm for the remainder of the run. The Mn increased to 140 ppm after 3150 hr of operation and remained at this value until 3600 hr, when it de-

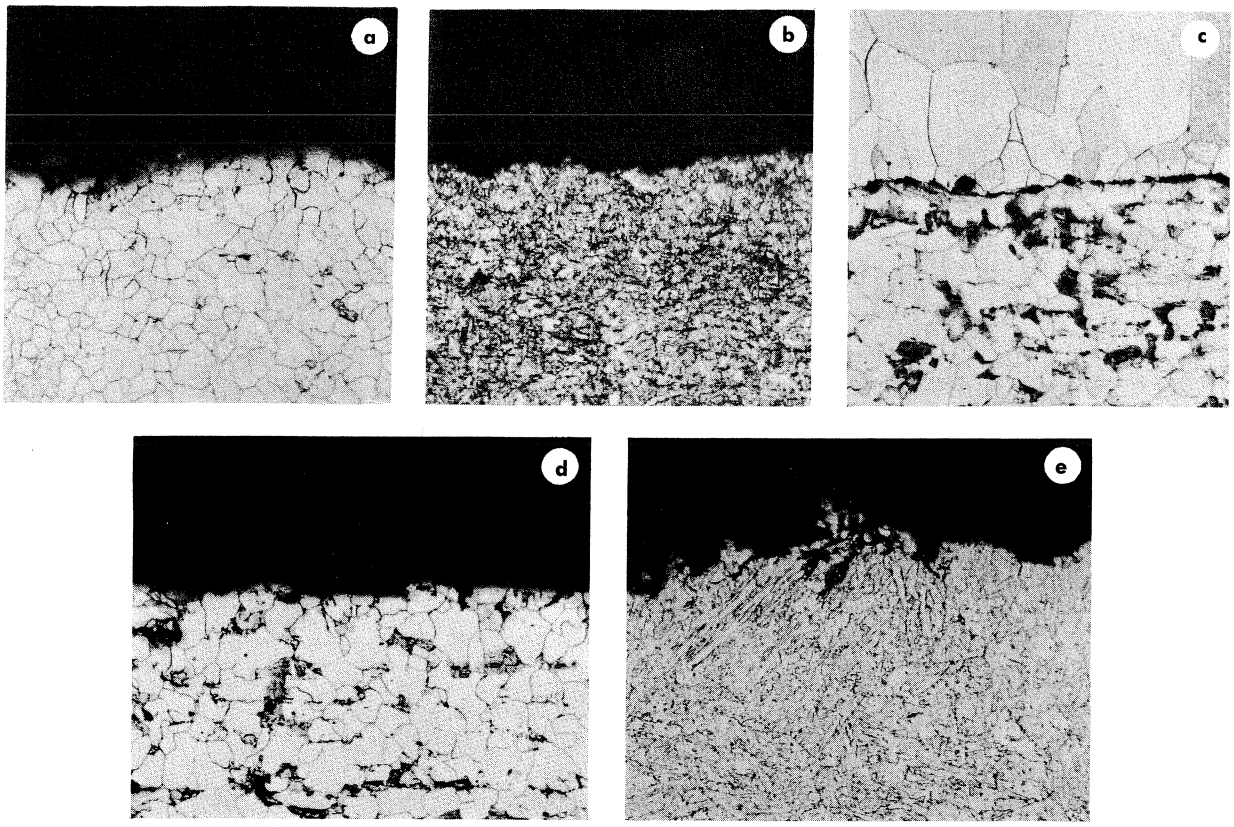

Figure 23. Photomicrographs (250×) of portions of thermal convection Loop L-7 (2¼ Cr – 1 Mo alloy steel). Nital etch. (a) Corrosion at bottom of surge tank. (b) Polished test specimen showing transgranular and slight intergranular corrosion. (c) Deposition and slight corrosion of section of pipe between surge tank and cold leg. (d) Corrosion at bottom of cold leg. (e) Corrosion of a weld.

creased for an unknown reason to 60 ppm; it then increased slowly to its final concentration of 95 ppm. Ni was not detected (limit of detection 10 ppm).

Visual inspection of the loop revealed no extensive corrosion. Microscopic examination showed a general state of transgranular and slight intergranular corrosion throughout the loop and surge tank (Figure 23). Corrosion in the lower section of the hot leg reached a maximum depth of 2.2 mils and an average attack of 1.5 mils. The polished standard section showed corrosion from 0.8 mil average to 1 mil maximum. The pipe leading from the surge tank to the cold leg exhibited an average attack of 0.8 mil and a maximum of 1.9 mils. Corrosion was also evident in the bottom of the cold leg, where attack reached a maximum of 1.5 mils and an average of 1 mil. Deposition was noted in several areas of the cold leg and throughout the hot leg. Chemical analysis showed the plug material to be principally Fe combined with $\approx$2% Cr.

The weld corrosion was not significantly greater than that in any other region in the loop. Maximum attack was 2.4 mils.

The corrosion in the loop tests was low, and welds were not preferentially attacked in any of them. The highly polished test specimen surfaces corroded appreciably less than the corresponding pipe surfaces which had been sandblasted prior to assembly. The compositions of the deposits were similar to those of the original steel.

FORCED CIRCULATION LOOP TEST

Some information on corrosion by the ternary eutectic was obtained from the operation of a mechanical components test loop (Figure 24) made of type 347 stainless steel. The loop was operated iso-

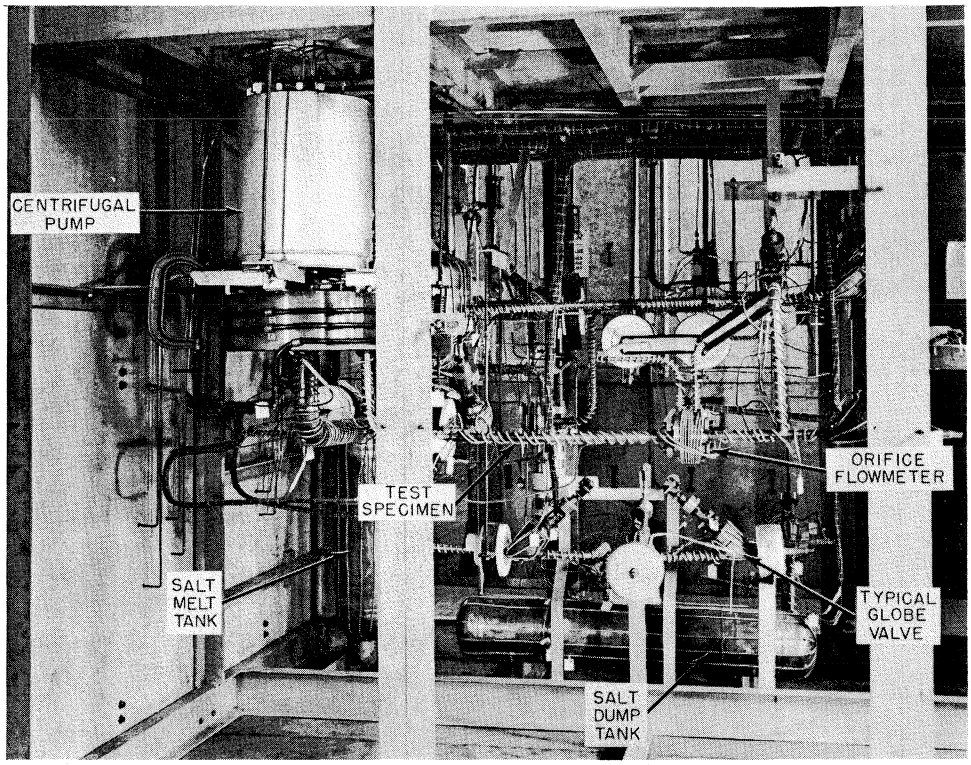

Figure 24. Photograph of fused salt forced circulation Loop M taken prior to application of insulation.

thermally at velocities of 2 to 13 ft/sec. In the first of two tests (see Table 8), which were primarily pump tests, the salt was circulated for 1034 hr at 520°C and a maximum velocity of 13.2 ft/sec. Upon conclusion of the test, a ½-in. IPS polished test specimen was removed from the loop and examined metallographically. Slight transgranular attack (1.3 mils/year maximum penetration) was found (Figure 25a).

The loop was sampled periodically during the first run, and the salt was analyzed for corrosion products. The Ni concentration remained constant at 10 ppm for the entire test, and the Mn concentration increased slightly from 10 to 21 ppm. The Cr concentration increased rapidly from 23 to 90 ppm in the first 80 hr and then more slowly to 155 ppm, and Fe increased from 10 to 800 ppm.

In the second test the salt was circulated for 656 hr at 515°C at velocities varying from 1.8 to 7.9 ft/sec. A section of ½-in. pipe, whose surface had been sandblasted during fabrication, was removed and examined. Transgranular attack (10.8 mils/year maximum penetration) was found (Figure 25b). As in the case of the thermal convection loops, the corrosion of highly polished metal surfaces in this loop was appreciably less than that of sandblasted ones.

SUMMARY OF RESULTS

The NaCl-KCl-$MgCl_2$ eutectic by itself was tested in all apparatus types with a wide variety of metallic materials and some ceramics. With few exceptions, it produced little corrosion. Weld areas were not preferentially attacked. The extent of mass transfer attack by the eutectic was negligible in 1000-hr tilting-furnace capsule tests, but plugging did occur in the type 410 stainless steel thermal convection loop after 4000 hr of operation. Little or no Ni was found in corrodent analyses in any of the tests of Ni-bearing alloys. This suggests that further studies might show high Ni alloys to be superior to all others tested here.

The tests reported here do not clearly show a superior container material or particular range of superior container material compositions for the ternary eutectic. Hence, a wide variety of materi-

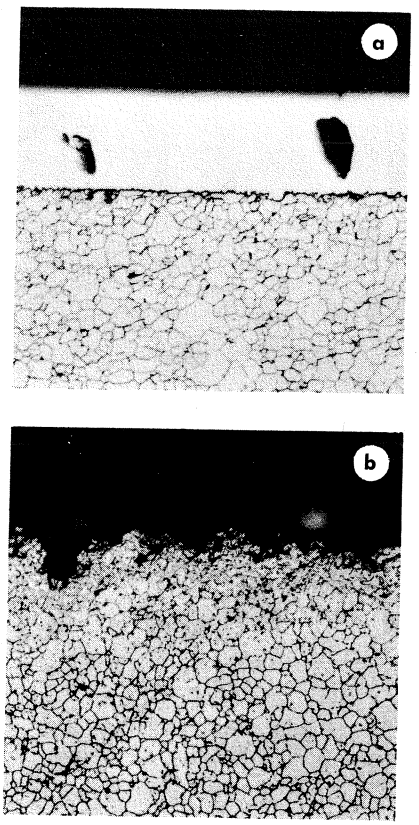

Figure 25. Photomicrographs (250×) of portions of forced circulation Loop M (type 347 stainless steel). Marbles etch. (a) Surface of polished test section. (b) Surface of ½-in. pipe.

als is available for further study and experimental use.

The fact that the ternary eutectic produced little corrosion, plus the observation that on completion of the tests there was generally no evidence of discoloration due to rust within the test apparatus, indicates that the methods of corrodent purification and handling were effective and that the different types of apparatus were leak tight.

Corrosion by the liquid metal – fused ternary salt system in the absence of $BiCl_3$ resembled that expected in the presence of fuel alone. Alloys resistant to fuel were found to be resistant to fuel in the presence of salt. The selection of a container material for the two-phase system thus appears to hinge on the selection of a container material for fuel. At present, 1020 mild steel, 1¼ Cr – ½ Mo, or 2¼ Cr – 1 Mo are most likely to be used for this purpose.

The facts that, on completion of the experiments, the container surfaces were found to be wetted by the Bi, and salt was never found at the Bi-container interface, suggest that creep of salt into the fuel system via such interfaces will probably not occur in a processing plant.

In the presence of liquid metal fuel and 5% $BiCl_3$ in ternary eutectic, both materials tested, Mo and Ta, were subject to transgranular attack, and the $BiCl_3$ was almost completely reduced. However, in these tests $BiCl_3$ was present stoichiometrically in excess of the oxidizable fuel solutes, U, Mg, and Zr. When U, Mg, and Zr are present in stoichiometric excess of $BiCl_3$, it has been found in other work at Brookhaven[11] that the fuel solutes are oxidized and not the container material. This has been found to be true in repeated experiments involving type 347 stainless steel and Mo containers. Thus it appears that contacting vessels in a processing plant in which $BiCl_3$ will be present may be made of materials selected primarily for resistance to fuel, as long as $BiCl_3$ is not in excess of oxidizable fuel solutes. Such is the case in the process flow sheet (Figure 1).

The principal corrosion problem in the process appears to be that of containing solutions of $BiCl_3$ in eutectic from the point of make-up to the point of consumption. Although Al_2O_3 and Au withstood attack by this corrodent in capsule experiments, further experiments, on a larger scale, would be required before they could be recommended as practical materials of construction.

In all tests, mechanically polished surfaces generally withstood attack better than sandblasted surfaces.

The LiCl-KCl eutectic was tested by itself in a few early experiments involving static capsules and thermal convection loops. Like the ternary eutectic, it proved to be a mild corrodent.

ACKNOWLEDGMENTS

The authors gratefully acknowledge the contributions of the following Brookhaven National Laboratory staff members and groups: G. Farber and W. Hansen in the development of experimental techniques and for conducting experiments; O.E. Dwyer and J.R. Weeks for their helpful suggestions and advice; the Metallography Section for examining the corrosion specimens; and the Hot Laboratory Radiochemical Analysis Section for analyzing the corrodents. The ceramic and Inor-8 test materials were supplied by the Norton Company and Oak Ridge National Laboratory, respectively.

REFERENCES

1. O.E. Dwyer, A.M. Eshaya, and F.B. Hill, Continuous removal of fission products from uranium-bismuth reactor fuels, *Proc. 2nd UN Intern. Conf. on Peaceful Uses of Atomic Energy,* Vol. 17, pp. 428-37, UN, Geneva, 1958.
2. *Report of the Fluid Fuel Reactors Task Force to the Division of Reactor Development, US AEC,* TID-8507, Feb. 1959.
3. D.W. Bareis, *A Continuous Fission Product Separation Process. 1. Removal of the Rare Earths (Lanthanum, Praseodymium and Neodymium) from a Typical Liquid Bismuth-Uranium Reactor Fuel by Contact with Fused LiCl-KCl Mixtures, LFR-3,* BNL 125, July 1951, Declassified March 1957.
4. C. J. Klamut, D.G. Schweitzer, J.G.Y. Chow, R.A. Meyer, O.F. Kammerer, J.R. Weeks, and D.H. Gurinsky, Material and fuel technology for an LMFR, *Proc. 2nd UN Intern. Conf. on Peaceful Uses of Atomic Energy,* Vol. 7, pp. 173-95, UN, Geneva, 1958.
5. J.H. Jackson and M.H. LaChance, Resistance of cast Fe-Ni-Cr alloys to corrosion in molten neutral heat treating salts, *Trans. Am. Soc. Metals* **46**, 157-83 (1954).
6. M.A. Bredig, J.W. Johnson, and W.T. Smith Jr., Miscibility of liquid metals with salts. I. The sodium-sodium halide systems, *J. Am. Chem. Soc.* **77**, 307-12 (1955).
7. *Brookhaven National Laboratory Nuclear Engineering Department Progress Report, April 16 – November 15, 1955,* BNL 380.
8. R.W. Fisher and G.R. Winders, High temperature loop for circulating molten metals, Paper No. 26, A.I. Ch.E. Annual Meeting, Nov. 29, 1955.
9. C. J. Raseman, H. Susskind, G. Farber, W.E. McNulty, and F. J. Salzano, *Engineering Experience at Brookhaven National Laboratory in Handling Fused Chloride Salts,* BNL 627 (T-192), June 1960.
10. C. J. Raseman and J. Weisman, *Liquid Metal Fuel Reactor Processing Loops, Part I,* BNL 322 (T-55), June 1954.
11. F. J. Salzano and F.B. Hill, Unpublished work at BNL, 1958.
12. J. Forrest and H.L. Finston, The spectrochemical analysis of bismuth using a photoelectric spectrometer, *Appl. Spectroscopy* **14**, 127-30 (1960).
13. J. Forrest, BNL, Private communication, 1960.
14. E.B. Sandell, *Colorimetric Determination of Traces of Metals,* Second Edition, Interscience, New York, 1950.
15. L. Newman, BNL, Private communication, 1960.
16. J.H. Yoe, F. Weill III, and K.A. Block, *Anal. Chem.* **25**, 1200 (1953).
17. R.W. Stoenner, BNL, Private communication, 1960.

APPENDIX A

Mill Test Reports of Metallic Materials Tested

(Composition in weight %)

	Cr	Ni	Fe	Mo	P	C	Cu	Si	S	Mn
Inor-8[a]	6.99	70.50	4.85	15.82	0.009	0.02	0.03	0.32	0.014	0.34
Hastelloy C[b]	15.63	Balance	6.57	15.43	0.012	0.05	—	0.48	0.006	0.48
Inconel	15.76	75.91	7.34	—	—	0.04	0.17	0.18	0.007	0.23
S.S. 304 (ELC)	18.37	10.51	Balance	0.01	0.02	0.03	0.12	0.47	0.09	1.17
S.S. 310	25.19	21.52	"	0.12	0.022	0.038	0.20	0.28	0.004	1.73
S.S. 316	16.99	13.25	"	2.32	0.022	0.05	—	0.68	0.015	1.86
S.S. 347[c]	17.49	11.4	"	0.23	0.019	0.051	0.19	0.54	0.007	1.71
S.S. 410	12.39	0.21	"	0.08	0.021	0.13	0.14	0.37	0.012	0.70
S.S. 430	16.79	0.31	"	—	0.02	0.072	—	0.18	0.01	0.35
S.S. 446	26.50	0.22	"	—	0.014	0.10	0.176	0.72	0.006	0.58
5 Croloy[d]	5.0	—	"	0.5	0.02	0.1	—	0.5	0.02	0.45
16-1 Croloy	16.64	0.85	"	0.02	0.016	0.02	0.13	0.20	0.02	0.57
2¼ Cr – 1 Mo	2.30	—	"	1.03	0.016	0.11	—	0.37	0.016	0.46
1¼ Cr – ½ Mo	1.10	—	"	0.54	0.017	0.11	0.05	0.55	0.011	0.39
1020 Mild steel[d]	—	—	"	—	0.04[m]	0.20	—	—	0.05[m]	—
Gold[e]	—	—	—	—	—	—	—	—	—	—
Molybdenum[d]	—	0.02[m]	0.005	99.9	0.03	—	—	—	—	—
Tantalum[f]	—	—	0.03	—	—	0.03	—	—	—	—
Stellite-90[g]	27	—	Balance	—	—	2.75	—	1[m]	—	1[m]

[a]Also contains Co, 0.51; W, 0.35; B, 0.04.
[b]Also contains W, 3.86; V, 0.24.
[c]Also contains Cb, 0.68; Te, 0.049.
[d]Nominal composition.
[e]Nominal composition: Au, 99.9+; Ag, 0.02; Cu, 0.002.
[f]Nominal composition: Ta, 99.9.
[g]Also contains 3% trace elements consisting of Mo, Ni, and Co.
[m]Maximum.

APPENDIX B

CHEMICAL ANALYSIS OF BI-U FUEL AND FUSED SALT SOLUTIONS

The following methods were used to measure the concentrations of corrosion products (Fe, Cr, Mn, Ni, Mo, and Ta) and additives (U and Zr) in the Bi-U fuel and fused salt solutions, of Mg in Bi-U fuel solution, and of Au and $BiCl_3$ (as Bi) in the fused salt.

Procedures were developed at Brookhaven to analyze for Fe, Cr, Mn, and Ni in both Bi[12] and fused salt,[13] for Mg and Zr in Bi,[12] and for Zr in fused salt[13] with the emission spectrograph. Solution techniques were used in all cases. The lower limits of detection are 10 ppm for corrosion products, 10 ppm for Mg in Bi, 50 ppm for Zr in Bi, and 20 ppm for Zr in fused salt.

The concentration of Mo in the fused salt was determined by the spectrophotometric thiocyanate-$SnCl_2$ method.[14] The addition of copious quantities of NH_4Cl permitted the method to be used also for the analysis of Mo in Bi-U fuel solution. The lower limit of detection is 5 ppm.

The Ta concentration in both the fused salt and the Bi-U fuel solutions was determined with the emission spectrograph, with Nb used as a carrier and also as an internal standard.[15] In the analysis for Ta in Bi-U fuel, the Bi had to be separated from the combined Nb-$Bi(OH)_3$ precipitate; this was accomplished by addition of NH_4Cl and volatilization of the $BiCl_3$ formed. The lower limit of detection is 10 ppm.

The Au concentration in the fused salt was measured by the $SnCl_2$ method,[14] in which a solution of colloidal Au is obtained and analyzed spectrophotometrically. The lower limit of detection is 0.1 ppm.

The concentration of $BiCl_3$ (as Bi) in the fused salt was determined by the spectrophotometric BiI_3 method,[14] which permits analysis down to 0.05%.

U was determined in both Bi and fused salt by the spectrophotometric dibenzoylmethane method of Yoe et al.,[16] as modified by Stoenner of the Brookhaven Chemistry Department.[17] The lower limit of detection is 10 ppm.

APPENDIX C

AXIAL TEMPERATURE PROFILE OF TILTING-FURNACE CAPSULE

The axial temperature profile of a typical capsule was measured by means of thermocouples inserted into wells adjacent to the two skin thermocouples at either end of the capsule and in wells at 5 intermediate points. The hot and cold end temperatures were controlled as described in the main body of the report. The thermocouples from all 7 thermowells were connected through a selector switch to a Brown strip chart recorder. Figure 26 is a representation of the temperature levels and temperature fluctuations obtained at each point. It may be seen that the hottest part of the capsule was at a temperature of about 525°C – not 500°C as desired – and this was not at the control point but at the midpoint of the capsule. The temperature difference between the hottest and coldest part of the capsule was therefore about 75°C rather than 50°C; however, the temperature difference between the tab and the coldest point was 50°C.

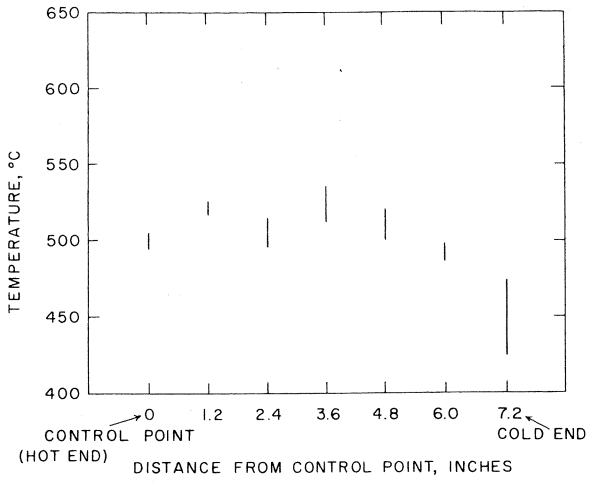

Figure 26. Axial temperature profile of a tilting-furnace capsule. Variation of the temperature at each point of measurement over a complete tilting cycle is indicated.

APPENDIX D

Crimping Forces Used in Tilting-Furnace Capsule Preparation (with 1.544-in.-diameter hydraulic ram)

	Force, lb
Flat Crimps	
All materials	16,000
Sharp Crimps	
Type 304 (ELC) S.S.	12,000
Hastelloy C (heated to dull red to prevent cracking)	12,000
Type 310 S.S.	8,000
Type 316 S.S.	8,000
Type 347 S.S.	8,000
Type 410 S.S.	8,000
Type 430 S.S.	8,000
16-1 Croloy	8,000
Type 446 S.S.	8,000
Inconel	8,000
Inor-8	8,000
2¼ Cr – 1 Mo Steel	8,000
1¼ Cr – ½ Mo Steel	8,000
Tantalum	5,000

APPENDIX E

TEST DATA AND RESULTS FOR TILTING-FURNACE CAPSULE SCREENING TESTS

Corrodent: NaCl-KCl-$MgCl_2$ Eutectic

Material	1020 Mild Steel		2¼ Cr – 1 Mo				304 (ELC) S.S.	
Sample No.	T-12[a]	T-13[a,b]	J-12[b]	J-13[b]	J-16[b,c]	J-17[b,c]	A-12	A-13
Av. hot end T, °C	500	500	502	502	500	500	501	501
Av. ΔT, °C	50	50	50	50	50	50	52	52
Outgassing T, °C	550	550	550	550	550	550	550	550
Outgassing time, hr	5	5	4	4	17	17	4	4
Length of test, hr	1000	1000	1000	1000	2500	2500	1000	1000
Weight loss of tab, %	0.286	+0.05	+0.22	+0.24	+2.3	+1.1	0.39	0.08
Weight loss of tab, mg/cm²	2.9	+0.49	+1.34	+1.46	+12.3	+6.0	2.27	0.49
Polished side of tab								
Type of corrosion	None	None	I&T*	I&T	None	None	I	I
Max. penetration, mils	0	0	0.38	0.30	0	0	<0.05	<0.05
Salt analysis, ppm								
Ni	—	—	—	—	—	—	24	<10
Cr	—	—	640	790	820	440	600	520
Fe	130	107	63	265	330	590	163	18
Mn	183	142	114	122	440	590	147	158

Material	310 S.S.		316 S.S.		347 S.S.		410 S.S.	
Sample No.	B-14[d]	B-15[d]	C-12	C-13[d]	D-12[d]	D-15[d]	E-12[d]	E-13[e]
Av. hot end T, °C	503	501	503	501	501	501	503	501
Av. ΔT, °C	52	51	52	51	51	51	52	51
Outgassing T, °C	550	550	550	550	550	550	600	550
Outgassing time, hr	8	4	4	4	4	4	4	4
Length of test, hr	1000	1000	1000	1000	1000	1000	1000	1000
Weight loss of tab, %	0.10	0.10	0.10	0.13	0.25	0.10	0.12	0.16
Weight loss of tab, mg/cm²	0.32	0.32	0.29	0.36	0.75	0.29	0.35	0.6
Polished side of tab								
Type of corrosion	None	None	I	I	I&T	I&T	I	I
Max. penetration, mils	0	0	<0.05	<0.05	0.60	0.46	0.08	0.15
Salt analysis, ppm								
Ni	<10	<10	<10	11	<10	<10	12	<10
Cr	>300	61	>250	>250	570	173	>300	>300
Fe	54	33	29	37	21	24	75	42
Mn	105	56	127	88	141	75	70	85

*I = intergranular; T = transgranular.

[a]Inside surface of capsule showed more corrosion than polished side of tab.

[b]Metal deposited on tab.

[c]Inside surface of capsule decarburized.

[d]Light rusting at cold end of capsule, probably due to Fe deposition.

[e]Plug at cold end of capsule.

Corrodent: $NaCl-KCl-MgCl_2$ Eutectic (continued)

Material	430 S.S.		16-1 Croloy		446 S.S.		Inconel	
Sample No.	N-12	N-13	M-12	M-13[f]	F-12[e]	F-13[e]	G-12	G-13
Av. hot end T, °C	501	501	501	501	501	501	503	501
Av. ΔT, °C	52	52	52	52	51	51	52	51
Outgassing T, °C	550	550	550	550	600	550	550	550
Outgassing time, hr	4	4	4	4	4	4	4	4
Length of test, hr	1000	1000	1000	1000	1000	1000	1000	1000
Weight loss of tab, %	0.03	0.02	+0.39	+0.01	+0.07	0.20	0.13	0.08
Weight loss of tab, mg/cm²	0.115	0.075	+1.86	+0.58	+0.34	0.62	0.45	0.27
Polished side of tab								
Type of corrosion	None	I	I	I	I	I	None	I
Max. penetration, mils	0	0.2	<0.05	<0.05	<0.05	<0.05	0	0.4
Salt analysis, ppm								
Ni	17	60	—	—	—	—	26	25
Cr	80	70	153	350	>1000	>1000	240	240
Fe	47	75	24	36	61	33	16	19
Mn	19	20	88	97	143	48	19	19

Material	Inor 8		Mo		Ta			
Sample No.	P-12	P-13[a,e]	K-12	K-13	L-14	L-15	L-18[a]	L-19[a]
Av. hot end T, °C	505	505	505	505	504	504	502	502
Av. ΔT, °C	53	53	54	54	51	51	48	48
Outgassing T, °C	550	550	550	550	550	550	550	550
Outgassing time, hr	3.5	3.5	3	3	4	4	4.5	4.5
Length of test, hr	1000	1000	1000	1000	1000	1000	1000	1000
Weight loss of tab, %	0.02	0.01	0.14	†	0.05	0.03	0.05	0
Weight loss of tab, mg/cm²	†	†	0.32	†	0.18	0.11	0.17	0
Polished side of tab								
Type of corrosion	T	None	None	None	I	I	None	None
Max. penetration, mils	0.46	0	0	0	1.2	<0.05	0	0
Salt analysis, ppm								
Ni	17	60	—	<10	—	—	—	—
Cr	80	70	—	17	—	—	—	—
Fe	47	75	14	113	—	—	—	—
Mn	19	20	—	—	—	—	—	—
Mo	—	—	600	600	—	—	—	—
Ta	—	—	—	—	32	51	160	150

†Not measured.
[f]Possibility of air contamination during sealing.

Welded Tab Specimens; Corrodent: NaCl-KCl-$MgCl_2$ Eutectic

Material	2¼ Cr – 1 Mo		347 S.S.		446 S.S.		Inconel	
Sample No.	J-22[g,h]	J-23[g,h]	D-20[h,i]	D-21[h,i]	F-18[h,j]	F-19[h,j]	G-14[h,k]	G-15[h,k]
Av. hot end T, °C	503	503	503	503	501	501	501	501
Av. ΔT, °C	56	56	56	56	50	50	50	50
Outgassing T, °C	500	500	500	500	500	500	500	500
Outgassing time, hr	14	14	8	8	5	5	16	16
Length of test, hr	2500	2500	2500	2500	2500	2500	2500	2500
Weight loss of tab, %	+0.94	+1.79	0.16	0.07	+0.2	2.76	0	+0.1
Weld								
Type of corrosion	I&T	I&T	T	None	I&T	I	T	T
Max. penetration, mils	<0.05	<0.05	0.12	0	0.05	0.05	0.2	0.2
Polished side of tab								
Type of corrosion	T	T	T	T	T	T	T	T
Max. penetration, mils	<0.05	<0.05	0.2	0.2	0.1	<0.05	0.1	0.2
Salt analysis, ppm								
Ni	<10	<10	<10	<10	<10	<10	<10	<10
Cr	391	>500	465	405	>500	>500	350	285
Fe	130	350	123	59	135	73	33	22
Mn	173	400	145	123	94	77	12	<10

[g]Tab weld was stress relieved at 725°C for 1 hr.
[h]The inside surface of the capsule showed nominal attack, similar to that indicated in the table for nonwelded tabs.
[i]Tab weld was stress relieved at 825°C for ½ hr.
[j]Tab weld was stress relieved at 750°C for 2 hr.
[k]Tab weld was stress relieved at 915°C for ½ hr.

Corrodent: Bi-U Fuel (1000 ppm U, 350 ppm Zr, 350 ppm Mg) and Ternary Eutectic								
Material	1020 Mild Steel		2¼ Cr – 1 Mo				304 (ELC) S.S.	
Sample No.	T-10	T-11	J-10	J-11	J-14[c]	J-15[c]	A-10[1]	A-11[1]
Av. hot end T, °C	502	502	500	500	504	504	500	500
Av. ΔT, °C	51	51	54	54	51	51	50	50
Outgassing T, °C	550	550	700	700	550	550	850	850
Outgassing time, hr	5	5	3	3	17	17	4	4
Length of test, hr	1000	1000	1000	1000	2500	2500	1000	1000
Weight loss of tab, %	+0.048	+0.037	+0.1	+0.04	+0.049	0	0.21	0.22
Weight loss of tab, mg/cm²	+0.41	+0.36	+0.65	+0.23	+0.33	0	1.16	1.07
Polished side of tab								
Type of corrosion	None	None	None	I	None	None	I	T
Wetting	Yes	No	No	No	Yes	Yes	Yes	Yes
Max. penetration, mils	0	0	0	<0.05	0	0	1.4	2.0
Sandblasted side of tab								
Type of corrosion	None	None	None	I	None	None	T	T
Wetting	Yes	No	No	No	Yes	Yes	Yes	Yes
Max. penetration, mils	0	0	0	<0.05	0	0	1.1	0.80
Inside capsule surface								
Type of corrosion	None	None	None	None	None	None	†	†
Wetting	No	No	No	No	No	No	Yes	Yes
Max. penetration, mils	0	0	0	0	0	0	†	†
Bismuth analysis, ppm								
U	579	157	481	271	546	563	161	247
Zr	168	0	132	<50	132	138	100	96
Mg	17	<10	88	<10	55	63	58	11
Fe	<10	<10	12	12	45	11	<10	11
Cr	—	—	10	40	<10	<10	<10	<10
Ni	—	—	31	10	—	—	85	39
Mn	—	—	18	18	—	—	31	34
Mo	—	—	<5	<5	<10	<10	<5	<5
Salt analysis, ppm								
U	568	295	107	115	127	430	5	8
Zr	31	36	<20	<20	30	17	<20	<20
Fe	224	730	49	93	330	820	25	62
Mn	—	24	0	<10	0	33	<10	18
Cr	—	—	0	0	0	0	<10	18
Ni	—	—	0	<10	—	—	0	0
Mo	—	—	—	—	<10	<10	—	—
Approx. wt. of magnetic cold plug, g	0	0	0	0	0	0	0.1	0.1

[1]Corrosion was found in longitudinal weld of capsule.

Corrodent: Bi-U (1000 ppm U, 350 ppm Zr, 350 ppm Mg) and Ternary Eutectic (continued)

Material	310 S.S.		316 S.S.		347 S.S.			
Sample No.	B-12	B-13	C-10[m]	C-11[m]	D-10	D-11	D-13[n]	D-14[n]
Av. hot end T, °C	500	500	500	500	500	503	500	500
Av. ΔT, °C	53	53	52	52	50	48	52	52
Outgassing T, °C	850	850	850	850	900	900	825	825
Outgassing time, hr	3	3	6	6	4	3.5	4	4
Length of test, hr	1000	1000	1000	1000	1000	1000	1000	1000
Weight loss of tab, %	7.35	0.36	0.1	0.46	†	†	0.15	0.41
Weight loss of tab, mg/cm^2	22.3	1.07	0.28	1.34	†	†	0.43	1.2
Polished side of tab								
Type of corrosion	I&T	I&T	I	I	I	I	I	I
Wetting	Yes	No	No	Yes	Yes	Yes	No	Yes
Max. penetration, mils	1.26	0.2	<0.05	1.3	0.5	1.7	<0.05	0.8
Sandblasted side of tab								
Type of corrosion	I	I	I	I	I	I	I	I
Wetting	Yes	Yes	Yes	Yes	Yes	Yes	Yes	Yes
Max. penetration, mils	0.5	0.8	0.8	0.3	0.5	0.3	0.4	1.0
Inside capsule surface								
Type of corrosion	I	I	I	I	I	I	I	I
Wetting	Yes	Yes	Yes	Yes	Yes	Yes	Yes	Yes
Max. penetration, mils	1.1	0.3	0.95	0.8	0.6	0.3	0.1	1.0
Bismuth analysis, ppm								
U	18	190	257	271	672	743	269	348
Zr	<50	<50	84	117	265	230	127	233
Mg	208	322	138	<50	155	70	215	207
Fe	11	22	<10	<10	<10	<10	12	<10
Cr	19	27	10	10	<10	<10	10	<10
Ni	2900	1800	110	190	190	170	32	86
Mn	110	110	39	59	41	69	28	34
Mo	<5	<10	—	—	—	—	—	—
Salt analysis, ppm								
U	8	25	89	126	Lost	2	16	50
Zr	<20	<20	<20	<20	"	25	<20	20
Fe	12	17	34	43	"	65	22	27
Mn	20	<10	<10	11	"	<10	<10	<10
Cr	<10	<10	<10	<10	"	<30	<10	<10
Ni	<10	<10	<10	—	"	<25	<10	<10
Approx. wt. of magnetic cold plug, g	1.0	0.1	0	0	0	0	0.1	0.1

[m]Capsule was sectioned below the salt-Bi interface. No salt was observed at the Bi – metal wall interface.

[n]The capsule and one side of the tab were electropolished. The corrosion data for the electropolished side of the tab are listed under the head "Sandblasted side of tab."

Corrodent: Bi-U (1000 ppm U, 350 ppm Zr, 350 ppm Mg) and Ternary Eutectic (continued)

Material	410 S.S.		430 S.S.		16-1 Croloy		446 S.S.	
Sample No.	E-10	E-11	N-10	N-11	M-10°	M-11	F-10	F-11
Av. hot end T, °C	504	503	504	504	501	501	504	503
Av. ΔT, °C	50	48	52	52	52	52	50	48
Outgassing T, °C	900	900	550	550	550	550	850	850
Outgassing time, hr	4	4	4	4	4	4	10	3.5
Length of test, hr	1000	1000	1000	1000	1000	1000	1000	1000
Weight loss of tab, %	1.69	2.85	†	†	1.5	0.76	†	0.11
Weight loss of tab, mg/cm²	4.85	8.2	†	†	6.0	3.07	†	0.35
Polished side of tab								
Type of corrosion	I	I	I	I	I	I	None	None
Wetting	Yes	Yes	Yes	Yes	Yes	Yes	No	No
Max. penetration, mils	0.8	0.6	0.3	0.9	0.5	0.5	0	0
Sandblasted side of tab								
Type of corrosion	I	I	I	I	I	I	I	I
Wetting	Yes	Yes	Yes	Yes	No	No	No	No
Max. penetration, mils	1.1	0.8	0.4	0.4	0.4	0.2	0.1	0.2
Inside capsule surface								
Type of corrosion	I	None	I	I	I	I	†	I
Wetting	Yes	No	Yes	Yes	Yes	Yes	No	No
Max. penetration, mils	0.31	0	0.2	0.3	0.4	0.8	†	0.1
Bismuth analysis, ppm								
U	387	438	419	519	325	300	672	532
Zr	<50	<50	138	50	87	62	171	200
Mg	<50	64	171	207	35	220	101	123
Fe	<10	10	9	15	13	9	<10	<10
Cr	<10	<10	16	17	16	13	16	<10
Ni	25	26	18	13	25	21	20	<10
Mn	84	38	19	16	39	34	12	40
Salt analysis, ppm								
U	—	—	192	228	88	231	4	18
Zr	<20	<20	<20	<20	<20	<20	<10	29
Fe	80	24	67	51	34	35	30	290
Mn	19	<10	0	0	0	0	<10	19
Cr	<30	<20	<10	<10	12	<10	<30	115
Ni	<25	<25	0	0	0	0	<25	<25
Approx. wt. of magnetic cold plug, g	3	1	0.75	0.3	0.5	0.5	0	0.1

°Cold end of capsule was slightly oxidized before sealing.

Corrodent: Bi-U Fuel (1000 ppm U, 350 ppm Zr, 350 ppm Mg) and Ternary Eutectic (continued)

Material	Inconel		Hastelloy C		Inor 8		Mo		Ta	
Sample No.	G-10	G-11	H-10[q]	H-11[q]	P-10[r]	P-11[r]	K-10	K-11	L-12	L-13
Av. hot end T, °C	504	503	503	503	504	504	505	505	501	501
Av. ΔT, °C	50	48	53	53	52	52	51	51	49	49
Outgassing T, °C	850	850	850	850	550	550	550	550	850	850
Outgassing time, hr	3.5	3.5	6	6	4	4	3	3	4	4
Length of test, hr	1000	1000	1000	1000	1000	1000	1000	1000	1000	1000
Weight loss of tab, %	17.0	†	4.3	3.2	24.0	30.0	+0.02	†	0.43	0.10
Weight loss of tab, mg/cm²	60	†	14.7	22.2	107	121	+0.05	†	1.51	0.38
Polished side of tab										
Type of corrosion	I&T	I&T	I&T	I&T	I&T	I&T	None	None	T	T
Wetting	Yes	Yes	Yes	Yes	Yes	Yes	No	No	Yes	Yes
Max. penetration, mils	[p]	[p]	3.0	4.25	[p]	[p]	0	0	0.85	0.1
Sandblasted side of tab										
Type of corrosion	I	I	I	I	I&T	I&T	None	None	I	I
Wetting	Yes	Yes	Yes	Yes	Yes	Yes	No	No	Yes	Yes
Max. penetration, mils	1.1	0.8	1.8	1.7	[p]	[p]	0	0	0.3	1.6
Inside capsule surface										
Type of corrosion	I	None	I	I	I&T	I&T	None	None	I	I
Wetting	Yes	No	Yes	Yes	Yes	Yes	No	No	Yes	Yes
Max. penetration, mils	0.3	0	0.3	0.2	[p]	[p]	0	0	0.4	0.4
Bismuth analysis, ppm										
U	61	55	18	41	6	18	570	185	Lost	1.4
Zr	50	—	<50	<50	<30	<30	128	142	141	<30
Mg	386	354	126	10	397	569	92	192	32	<10
Fe	<100	400	18	9	28	13	14	57	—	—
Cr	<100	<100	15	15	10	32	—	—	—	—
Ni	1.6%	1.7%	4100	2800	16	>1000	—	—	—	—
Mn	90	90	30	40	0	>250	—	—	—	—
Mo	—	—	35	7	—	—	0	0	—	—
Ta	—	—	—	—	—	—	—	—	Lost	29
Salt analysis, ppm										
U	55	0.3	15	8	7	2	2	0.3	144	3076
Zr	<20	52	20	<20	<20	<20	<20	<10	17	123
Fe	49	46	16	18	<10	0	0	<10	—	—
Mn	<10	<10	0	<10	95	0	0	0	—	—
Cr	<30	<30	<10	<10	<10	<10	0	0	—	—
Ni	55	38	<10	<10	385	10	0	0	—	—
Mo	—	—	—	—	—	—	<100	<100	—	—
Ta	—	—	—	—	—	—	—	—	29	57
Approx. wt. of magnetic cold plug, g	12	12	0.5	0.5	†	†	0	0	0	0

[p]Corrosion was so extensive that it could not be measured accurately.
[q]Nonmagnetic cold plug was found.
[r]There was a cold plug in the capsule, but no estimate of its weight was made.

Corrodent: $NaCl-KCl-MgCl_2$ Eutectic Plus 4.76% $BiCl_3$

Material	Mo		Ta		Gold	
Sample No.	K-16[s,t]	K-17[s,t,u]	L-22[s,t,u]	L-23[s,t,u]	Au-1[v]	Au-2[v,w]
Av. hot end T, °C	503	503	503	503	503	503
Av. ΔT, °C	50	50	52	52	55	55
Outgassing T, °C	550	550	550	550	—	—
Outgassing time, hr	4	4	4.5	4.5	—	—
Length of test, hr	600	600	1600	1600	1000	1000
Weight loss of tab, %	†	†	2.5	2.2	0.131	0.116
Weight loss of tab, mg/cm²	†	†	8.7	7.8	0.33	0.3
Polished side of tab						
Type of corrosion	Pitting	Pitting	Pitting	Pitting	None	I
Max. penetration, mils	0.1	0.2	0.1	0.4	0	0.6
Salt analysis, ppm						
Mo	Lost	Lost	—	—	—	—
Ta	—	—	Lost	130	—	—
Au	—	—	—	—	15	15
$BiCl_3$	<0.05%	<0.05%	Lost	<0.05%	4.54%	5.3%

[s]Deposit of metallic Bi found on tab and inside surface of capsule.
[t]Run was terminated when glass sealing container was accidentally broken.
[u]Inside capsule surface showed pitting and/or intergranular corrosion.
[v]This was a glass capsule with a long Au tab running its length.
[w]The corrosion was found on the hot end of the long tab; none was found on the cold end.

Corrodent: Bi-U Fuel/Ternary Eutectic Plus 4.76% $BiCl_3$			
Material	Mo		Ta
Sample No.	K-14	K-15	L-20[x,y]
Av. hot end T, °C	502	502	502
Av. ΔT, °C	49	49	50
Outgassing T, °C	550	550	550
Outgassing time, hr	4	4	4.5
Length of test, hr	2500	2500	2500
Weight loss of tab, %	0.03	0.14	0.6
Weight loss of tab, mg/cm^2	0.074	0.58	2.3
Polished side of tab			
Type of corrosion	T	T	T
Max. penetration, mils	0.8	0.2	0.5
Bismuth analysis, ppm			
U	0	0	0
Zr	<50	<50	<50
Mg	<50	<40	<40
Mo	<10	<10	—
Ta	—	—	15
Salt analysis, ppm			
U	3540	3110	4150
Zr	1020	1050	—
Mo	1250	1420	—
Ta	—	—	390
$BiCl_3$	0.235%	0.375%	0.15%

[x]L-21, the duplicate of L-20, developed a crack in the glass enevelope and corroded because of air leakage. No results were obtained.

[y]The hot end of the inside capsule surface was corroded transgranularly and intergranularly. The maximum depth of penetration was 1 mil.

APPENDIX F

RESULTS OF THERMAL CONVECTION AND FORCED CONVECTION LOOP CORROSION PRODUCT ANALYSES

Sample	Time, hr	Fe, ppm	Cr, ppm	Mn, ppm	Ni, ppm
Corrodent: LiCl-KCl Eutectic; Loop L-1					
1	841.5	171	62	63	ND
2	865.5	49	83	37	ND
3	1343.5	69	42	68	ND
4	1511.5	99	93	62	ND
5	1871.5	146	113	62	ND
Corrodent: LiCl-KCl Eutectic; Loop L-3					
200	213	0.11%	21	95	ND
Corrodent: NaCl-KCl-$MgCl_2$ Eutectic; Loop L-5					
0	0	<10	12	ND	<10
1	19	29	68	<10	ND
2	139.2	740	97	10	<10
3	186.5	23	61	<10	ND
4	305.5	101	106	12	ND
5	358	80	84	10	ND
6	473	125	104	13	ND
7	528.3	885	108	15	ND
8A	605	96	119	14	ND
8B	689.7	103	131	13	ND
9	785.9	107	123	22	ND
10	857.2	206	150	14	ND
11	978	181	172	20	ND
12	1024.7	220	197	17	ND
13	1143.7	315	209	14	ND
14	1192	258	210	25	ND
15	1316.3	315	213	30	ND
16	1360.1	300	265	22	ND
17	1479.2	305	245	28	ND
18	1527.3	250	238	24	ND
19	1702.1	240	265	26	ND
20	1960.2	178	276	28	ND
21	2032.4	235	328	27	ND
22	2203.0	224	393	25	ND
Corrodent: NaCl-KCl-$MgCl_2$ Eutectic; Loop L-6					
2	355.6	500	205	<10	<10
3	420.4	555	145	13	<10
4	587.7	645	150	19	21
5	756.2	880	196	18	<10
6	924.4	650	287	17	<10
7	1092.7	465	365	19	10
8	1212.5	475	246	22	<10
9	1212.5	445	338	24	<10
10	1429.3	650	223	33	<10

Sample	Time, hr	Fe, ppm	Cr, ppm	Mn, ppm	Ni, ppm
Corrodent: NaCl-KCl-$MgCl_2$ Eutectic; Loop L-6 (continued)					
11	1601	≈2000	485	32	21
12	1787	980	525	32	<10
13	1908.3	710	570	36	<10
14	2102	610	≈600	37	ND
15	2268.6	680	700	46	34
16	2435.3	650	≈630	44	ND
17	2603.2	760	≈750	54	ND
18	2770.9	710	≈750	60	ND
19	2945	620	≈805	65	ND
20	3203.5	440	1000–1500	62	ND
21	3276	440	1000–1500	62	<10
22	3446.1	415	1000–1500	73	21
23	3900	130	1000–1500	81	<10
Corrodent: NaCl-KCl-$MgCl_2$ Eutectic; Loop L-7					
1	19.0	84	ND	ND	ND
2	67.5	116	ND	ND	ND
3	139.5	136	ND	ND	ND
4	210.2	194	ND	ND	ND
5	306.3	310	ND	ND	ND
6	378.1	750	ND	ND	ND
7	474.2	193	ND	ND	ND
8	710.9	620	44	<10	ND
9	779.4	≈1350	31	<10	ND
10	874.7	700	35	<10	ND
11	972.5	690	40	10	ND
12	1044.0	760	51	32	ND
13	1211.0	640	<10	<10	ND
14	1235.4	700	34	11	ND
15	1282.4	570	26	<10	ND
16	1456.0	1030	51	16	ND
17	1477.1	1300	63	14	ND
18	1548.0	1230	66	17	ND
19	1619.0	1200	66	15	<10
20	1715.9	1350	89	16	<10
21	1787.7	1380	90	21	ND
22	1884.9	1450	100	21	ND
23	1960.0	1320	102	19	ND
24	2058.1	1530	103	25	ND
25	2125.5	1600	137	27	ND
26	2218.9	1500	146	30	ND
27	2297.0	1300	112	31	ND
28	2392.2	1360	134	37	ND
29	2463.5	1450	147	36	ND
30	2555.4	1590	162	49	ND
31	2723.6	1380	223	49	ND
32	2893.4	2100	600	84	<10

Sample	Time, hr	Fe, ppm	Cr, ppm	Mn, ppm	Ni, ppm
Corrodent: NaCl-KCl-$MgCl_2$ Eutectic; Loop L-7 (continued)					
33	2965.0	1560	>2000	360	64
34	3060.0	1460	470	94	12
35	3138.3	1310	615	136	<10
36	3269.0	1430	555	132	<10
37	3315.3	1420	510	126	<10
38	3379.5	1500	500	143	<10
39	3449.9	1420	560	146	<10
40	3548.2	1460	565	142	<10
41	3622.3	1490	395	61	—
42	3716.0	1340	445	65	—
43	3787.2	1490	410	66	—
44	3916.1	1460	412	74	—
45	3956.3	1470	395	70	—
46	4078.5	1460	335	72	—
47	4123.1	—	—	72	<10
48	4222.9	1600	357	82	15
49	4290.0	1600	339	78	<10
50	4387.2		insufficient sample		
51	4461.9	1600	402	98	<10
52	4555.1	1700	403	92	<10
53	4627.8		insufficient sample		
54	4723.2	1620	373	89	<10
55	4794.8	1600	378	87	<10
56	4890.2	1700	395	91	<10
57	4977.0	1730	365	86	<10
58	5057.8	1740	383	90	<10
59	5129.9	1770	378	87	<10
60	5225.8	1780	433	—	<10
61	5297.9	1750	373	84	<10
62	5394.0	1730	403	96	<10
63	5561.2	1730	413	95	<10
64	5632.9	1760	377	94	<10
65	5728.9	1730	413	97	<10
66	5801.0	1770	395	98	<10
67	5897.5	1780	445	92	<10
68	5973.4	2080	411	94	<10
69	6066.8	2040	390	93	<10
70	6140.6	2160	405	95	<10
71	6237.0	2070	419	100	<10
72	6280.8	2120	420	98	<10
Corrodent: NaCl-KCl-$MgCl_2$ Eutectic; Loop M*					
Initial	—	21	23	10	10
1	24.9	28	69	10	<10
2	258.7	210	105	10	11
3	582.4	320	94	18	10
4	654.3	1375	180	23	20
5	752.8	415	122	16	16
6	796.4	720	180	14	<10
10	916.9	440	131	18	<10
11	1034.0	185	143	20	<10
12**	1034.0	≈1700	135	24	11

*For Loop M, time represents pump hours. The initial sample was taken from the pretreatment tank, all other samples from the surge tank.

**Filtered sample.